CHARACTERIZING WILDFIRE IN THE FRANK CHURCH WILDERNESS, IDAHO, BETWEEN 1972-2012

by

Abigail Christine Axness

A thesis

submitted in partial fulfillment

of the requirements for the degree of

Master of Science in Geoscience

Boise State University

August 2022

BOISE STATE UNIVERSITY GRADUATE COLLEGE

DEFENSE COMMITTEE AND FINAL READING APPROVALS

of the thesis submitted by

Abigail Christine Axness

Thesis Title: Characterizing Wildfire in the Frank Church Wilderness, Idaho, between 1972-2012

Date of Final Oral Examination: 15 June 2022

The following individuals read and discussed the thesis submitted by student Abigail Christine Axness, and they evaluated the student's presentation and response to questions during the final oral examination. They found that the student passed the final oral examination.

Jen Pierce, Ph.D.	Chair, Supervisory Committee
Nancy F. Glenn, Ph.D.	Member, Supervisory Committee
Mojtaba Sadegh, Ph.D.	Member, Supervisory Committee

The final reading approval of the thesis was granted by Jen Pierce, Ph.D., Chair of the Supervisory Committee. The thesis was approved by the Graduate College.

DEDICATION

To Bjorn and my family for helping me throughout this challenging pandemic.

ACKNOWLEDGEMENTS

I want to thank my advisor, Dr. Jen Pierce, and committee members, Dr. Nancy Glenn, and Dr. Mojtaba Sadegh, for their support, guidance, and enthusiasm throughout this research; the National Science Foundation's Boise State University, Bridge to Doctorate Fellows for their community, help, and advice I grew as a graduate student; and Jadelyn Abbott for her assistance and patience with the writing and revision process.

ABSTRACT

I examined wildfire characteristics in the Frank Church Wilderness, central Idaho, between 1972-2012. Studying fire characteristics in the Frank Church Wilderness provides an opportunity to understand the history of wildfires in a federally designated wilderness area, largely devoid of management impacts with limited human access and activity. The ~958,000-hectare Frank Church Wilderness area encompasses the Middle Fork Salmon River. Vegetation cover ranges from high elevation (~2500-3200 meters) mixed conifer forests in the headwaters to low-elevation (~600-1000 meters) sagebrush-steppe and ponderosa pine (*Pinus Ponderosa*) forests. The Frank Church Wilderness is defined as unmanaged because effective fire suppression (e.g., vehicle and air-assisted fire suppression), logging, road access, and motorized vehicle use are extremely limited; therefore, this area provides an excellent location to examine historical changes in wildfire characteristics in the absence of substantial management influence. Studies of wildfires in the Western USA show an increase in area burned in the past several decades; however, the root cause of the trend is attributed to both historical fire suppression and a warming climate.

This research aims to understand fire characteristics and their correlation with a warming climate in the Frank Church Wilderness. Our research questions are:

1. *How do landscape fire metrics relate to warming trends in an unmanaged wilderness?*
2. *How are landscape metrics of burned areas correlated with one another?*

As a proxy for the influence of warming and drying on vegetation, I use vapor pressure deficit (VPD), which measures air aridity and is the difference between moisture pressure in the air and its value at saturation. The study uses fire atlas data from 1972-2012, remotely sensed data, and historical VPD records to test correlations among climate aridity, burn area, and other fire metrics.

This analysis shows that burned area in the Frank Church Wilderness increased between 1972-2012 and is significantly correlated with VPD, indicating that fires become larger as aridity increases. Severe fire years with large burn areas include 1988, 2000, and 2008. This work supports studies that attribute the growth in burned areas (1972-2012) to background warming and drying.

I used FRAGSTATS software and landscape metric calculations in a pilot study to better understand the changes to wildfire shape and total area burned in the Frank Church Wilderness. FRAGSTATS show a high positive correlation (Pearson correlation coefficient of 0.57) between total area burned and VPD (p-value of 0.001). The number of patches also positively correlated with VPD (p-value of 0.002). The landscape shape index had a positive correlation (Pearson correlation coefficient of 0.48) to VPD with a p-value of 0.01. Perimeter-area fractal dimension index metric had a negative correlation (Pearson correlation coefficient of -0.38) with VPD with a p-value of 0.05.

While additional work is needed, the scientific and land management communities can benefit from the nuanced understanding of the relationship between climate aridity and burned landscape patterns in an unmanaged region.

TABLE OF CONTENTS

LIST OF TABLES

LIST OF FIGURES

LIST OF EQUATIONS

LIST OF ABBREVIATIONS

FCW	Frank Church Wilderness- River of No Return
VPD	Vapor Pressure Deficit
PCM	Pearson Correlation Matrix
NIFC	National Interagency Fire Center
ha	Hectares
NP	Number of patches
PD	Patch density
LPI	Largest patch index
ED	Edge density
AREA_MN	Mean patch size
AREA_AM	Area-weighted mean patch size
AREA_CV	Patch size coefficient of variation
GYRATE_MN	Mean radius of gyration
GYRATE_AM	Area-weighted mean radius of gyration
GYRATE_CV	Radius of gyration coefficient of variation
LSI	Landscape shape index
COHESION	Patch cohesion index
SHAPE_MN	Mean shape index
AI	Aggregation index
SHAPE_CV	Shape index coefficient of variation

FRAC_MN	Mean fractal dimension
FRAC_AM	Area-weighted mean fractal dimension
FRAC_CV	Fractal dimension coefficient of variation
PARA_MN	Mean perimeter-area ratio
PARA_AM	Area-weighted mean perimeter-area ratio
PARA_CV	Perimeter-area ratio coefficient of variation
CONTIG_MN	Mean contiguity index
CONTIG_AM	Area-weighted mean contiguity index
CONTIG_CV	Contiguity index coefficient of variation
PLADJ	Percentage of like adjacencies
IJI	Interspersion and juxtaposition index
SHEI	Shannon's Evenness index
PAFRAC	Perimeter-area fractal dimension index
CONTAG	Contagion index
TA	Total area

INTRODUCTION

The size, frequency, and severity of large forest wildfires in the Western USA (including the states of Arizona, California, Colorado, Idaho, Montana, Nevada, New Mexico, Oregon, Utah, Washington, and Wyoming) have increased. In 2020, > 2.5 million ha burned, with > 1.5 million ha in California (3.7% of the state) alone, which included five of the six largest fires burned in the state's history (NASA, 2020). Over 760,000 ha burned in Oregon and Washington in the same year (Higuera and Abatzoglou, 2020). In 2020 in Idaho, over 900 fires burned >121,500 ha of rangeland and forests (National Interagency Fire Center, NIFC, 2021). The ability to better predict fire across Idaho is crucial to environmental challenges such as adjusting to new climate conditions (Krawchuk et al., 2009).

As wildfires become more common and dangerous, it is essential to understand the complex dynamics of the wildfire system (Westerling et al., 2006). Idaho is in the top ten states with extreme wildfire risks and many properties within danger (Verisk, 2021). Wildfires threaten people and property due to population growth and the expansion of communities in wildland-urban interface areas (McCaffrey et al., 2020).

Our study connects past fire regimes in mixed conifer forests in an unmanaged wilderness, the Frank Church Wilderness (FCW), from 1972- 2012. Our research questions are: How do landscape fire metrics relate to warming trends in an unmanaged wilderness? Secondly, how are landscape metrics of burned areas correlated with one another? Vapor pressure deficit (VPD) measures aridity and is the difference between the

amount of moisture in the air and how much moisture the air can hold when it is saturated. The study uses VPD and fire atlas data (based on satellite observations) from 1972-2012, resulting in analyses of ~ 300 fires. FRAGSTATS software was used to test correlations of burned area, landscape metrics, and climate aridity from the fire atlas and VPD data.

The connection of FRAGSTATS landscape metrics to VPD is not well understood. FRAGSTATS software is designed to compute various landscape metrics for categorical map patterns. VPD data (collected May-September of each year) is used to identify and statistically compare to FRAGSTATS data.

While researchers have identified that wildfires are becoming larger and more severe, there is still a gap in research specific to understanding the role of climate and landscape change in high-elevation mixed conifer forests.

Outputs of this study include statistical data and interpretation of VPD and landscape metrics to improve our understanding of the fire characteristics of the FCW.

Study Area

The ~958,000 hectares (ha) FCW provides a location to study wildfire and landscape change in a largely unmanaged wilderness. This project focused on fire records in high-elevation lodgepole pine and mixed conifer forests within the FCW in central Idaho, USA (Figure 1). The fire polygons from the fire atlas (Figure 1) are within the FCW and categorized by years.

The absence of prior fire suppression and logging allows the examination of wildfire regimes without major management influence. The FCW is significant to this study as it has been almost unmanaged for about ~92 years. The FCW has cultural history

through Native American and Euro-American sites. Native American tribal history extends to at least 12,000 years before the present (USDA, 2022). Oral history and numerous sites with lithic scatter, historical villages, pictographs, and bighorn sheep hunting traps are in the FCW. Historically and today, the two tribal groups, the Shoshone-Bannock, and the Nez Perce, live and utilize resources within the FCW (USDA, 2022). Additionally, in the 1800s, fur trapping and later, the discovery of gold increased the population, leaving behind a trail of historic sites (USDA, 2022). This indicates a minimal amount of management practices.

The FCW is located in five national forests: Boise, Bitterroot, Nez Perce, Payette, and Salmon-Challis (USDA, 2021). Restrictions of the wilderness include no timber harvesting and no new roads, new landing strips, and new transport (motorized or mechanized), including motorboats (except on the Salmon River). Commercial enterprises (other than guides and outfitters) are also not allowed. Dredge or placer mining in the Salmon River, Middle Fork, and tributaries of the Middle Fork is not permitted. New permanent installation is not allowed; however, structures may be maintained for administrative or historical purposes (USDA, 2021).

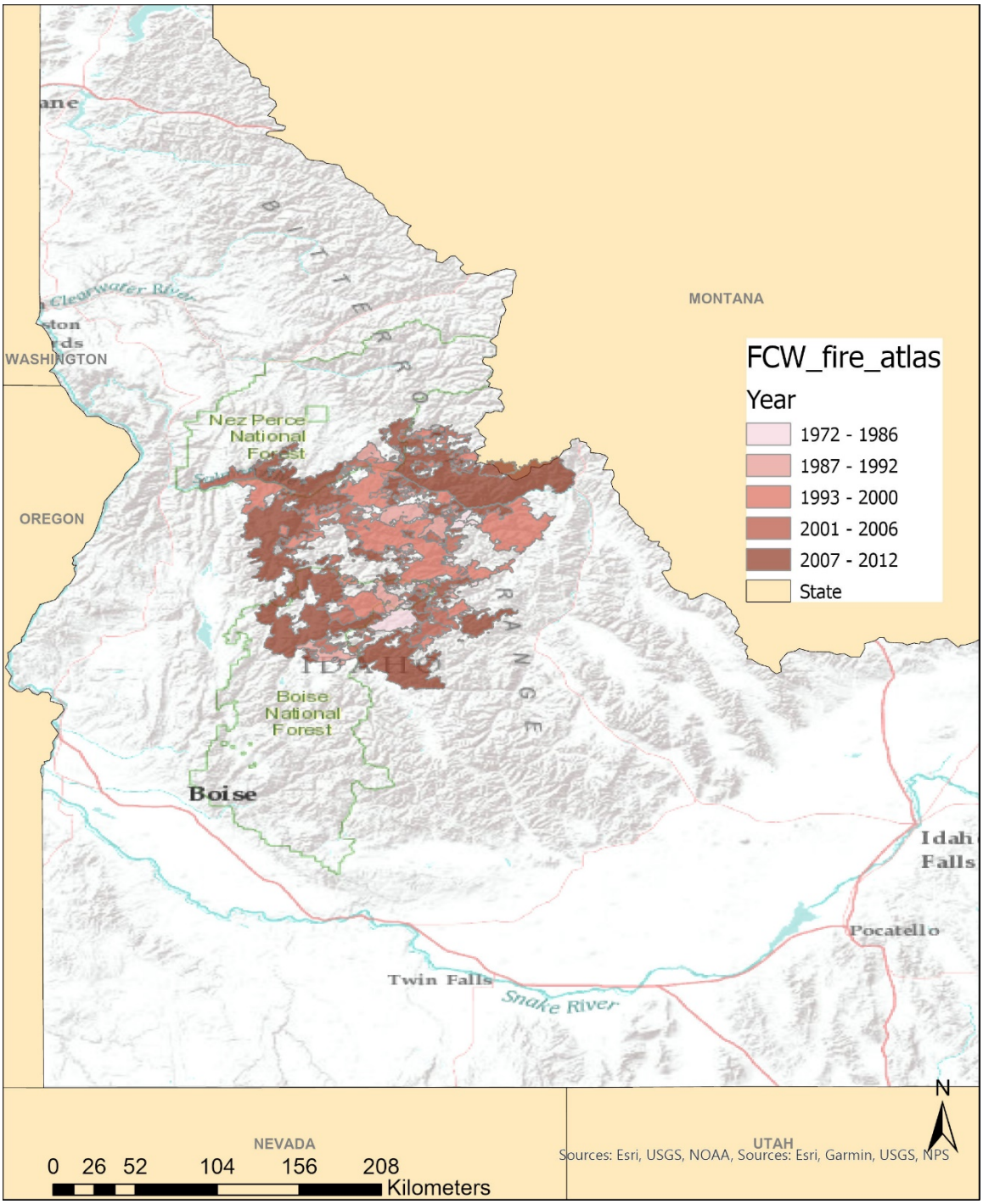

Figure 1. Map the State of Idaho and the Frank Church Wilderness (FCW) location. Fire perimeters within FCW are shown from 1972-2012.

Forest Types and Fire Regimes in the Frank Church Wilderness

Landscapes within FCW are at different stages of recovery because fire regimes are changing (Levin, 1976). The significant elevation range within FCW (600-3200 meters) encompasses a range of forest types, including high elevation mixed conifer and lodgepole pine-dominated forests, mid-elevation ponderosa pine (*Pinus Ponderosa*), and Douglas Fir (*Pseudotsuga Menziesii*) forests, and low elevation open ponderosa pine forests and sagebrush-steppe. This study focuses on high elevation mixed conifer forests. Historically (~1600-1900 AD), these forests experienced fire return intervals of ~200-400 years (Heyerdahl et al., 2019). These forests were 'moisture limited,' meaning they were historically too wet to burn during all but the driest years.

The Northern Rockies (including FCW) have experienced significant vulnerability to snowpack and changes in the timing of spring and snowmelt (Westerling et al., 2006). The western USA is heavily influenced by warming from early snowmelt and increased forest wildfire activity from warming (Heyerdahl et al., 2008).

A threshold at intermediate moisture conditions suggests that changes in vegetation from forest to shrubland/grassland are possible as the climate becomes warmer and drier (Parks et al., 2018). Significant changes in the distribution of specific vegetation types have meaningful interactions and feedbacks among climate, environment, fire, and vegetation (Parks et al., 2018). Limited anthropogenic burning within the FCW provides valuable insight into climate-driven wildfires.

Some key challenges, including longer wildfire seasons, and hotter and drier climates, contribute to the uncertainty of future effects of climate change. In addition, elevations above 2,500 meters are experiencing warmer conditions compared to previous

years (Alizadeh et al., 2021). A valuable visual representation of the upslope advancement of wildfires and anthropogenic warming is in Figure 2. Within Figure 2, the red and blue bars represent warmer and cooler temperatures, respectively, and over time, can mimic the elevation pattern as it changes as warmer (red) temperatures appear more frequently.

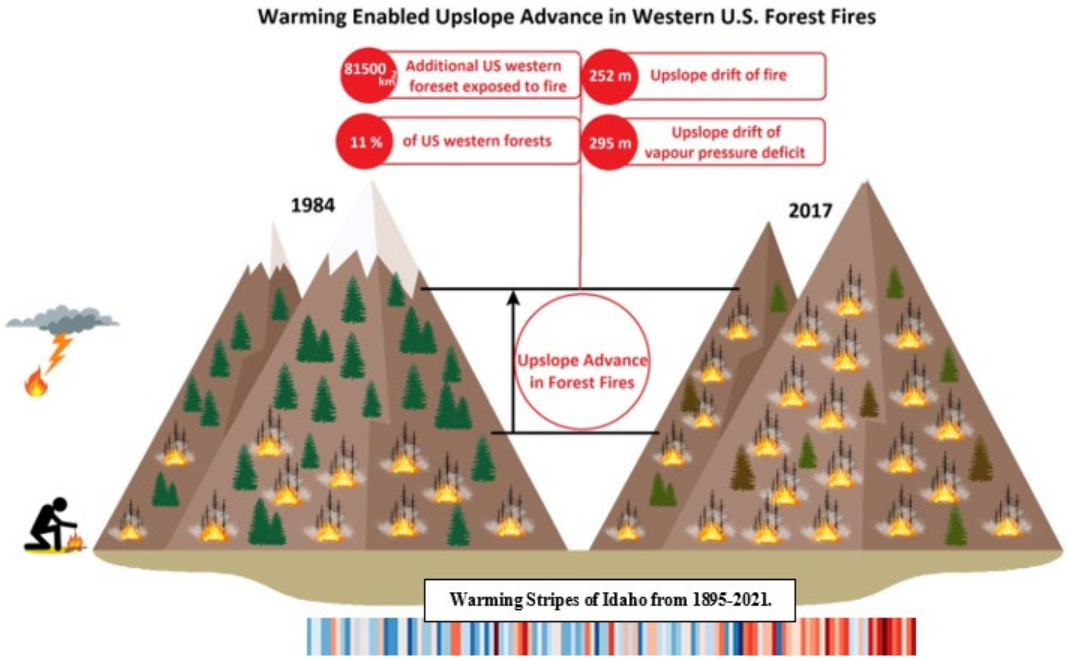

Figure 2. Elevation changes at 2,500 m (Alizadeh et al., 2021). Warming stripes of Idaho (1895-2021) (2022 Earth Stripes, 2022). Adapted from Alizadeh et al., 2021.

Background

Ostapowicz et al. (2008) used FRAGSTATS to calculate landscape metrics. Their study identified the analysis to connect landscape patterns with spatial patterns as having a strong correlation with pixel size and other connectivity features. The study also

deemed FRAGSTATS a powerful tool to study fire. Singleton et al. (2021) incorporated fire into the FRAGSTATS landscape metrics, demonstrating the tool's value.

VPD is the difference between the amount of moisture in the air and the moisture the air can hold (when saturated). High VPD will energize the evaporation of moisture, leaving forests and vegetation arid. Connecting VPD to landscape metrics provides valuable insight into our study location.

Fire Atlases

Fire atlases provide pyrogeography of fire regimes, including the spatial distribution of fire over time concerning landscape controls and climate (Morgan et al., 2014). The size and distribution of fires are valuable for understanding how fire regimes have changed over time (Rollins et al., 2001). Landscape controls on fire include total burned area by yearly totals; however, they can be done separately for each fire. Spatial data from fire atlases provide patterns of fire ages and extents in the FCW.

METHODS

Figure 3 outlines the methods used in this study, including the following steps: 1) classify the study area, 2) define the scale of the study area, 3) quantify the landscape composition and measure spatial configuration, and 4) identify unique landscape metrics and patterns. I used these steps to process each fire (see below) evaluated through FRAGSTATS.

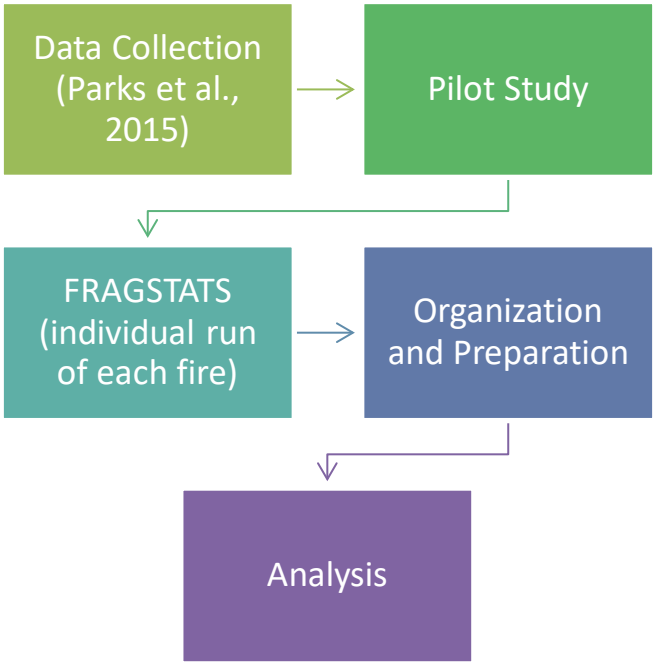

Figure 3. Flowchart of steps used for analysis.

Fire Atlas, 1972-2012 (Data Collection)

In this study, I used a fire atlas, "Quantifying the Effectiveness and Longevity of Wildland Fire as a Fuel Treatment" (Parks et al., 2015) (Figure 4), for 1972-2012 to generate fire perimeters. The fire atlas includes approximately 300 fires. The data from the fire atlas were then statistically evaluated using FRAGSTATS. Based on satellite-inferred metrics, the fire severity had all fires greater than or equal to 20 ha between 1972 and 2012 (Parks et al., 2015). I created a 10-year moving average interpretation of all fires that were >20 ha.

The two main components of the atlas include fire history shapefiles and raster files. A shapefile represents the fire perimeters, and the raster files represent satellite-inferred burn severity. The burn severity is measured as dNBR (delta normalized burn ratio), RBR (relativized burn ratio), and dNDVI (delta normalized difference vegetation index), which were calculated using Landsat TM (thematic mapper), ETM+ (enhanced thematic mapper plus), and OLI (operational land imager) data as part of the Parks et al. (2015) dataset.

Vapor Pressure Deficit (Data Collection)

I collected VPD data using the climate toolbox (Hegewisch et al., 2022) for the area of the FCW 1972-2012. The formula for VPD is presented in Equation 1.

$$VPD = e_s(T) - e_a = e_s(T)(1 - h_r)$$

T - at given air temperature
e_s – saturation vapor pressure (kPa)
e_a – vapor pressure
h_r – relative humidity

Equation 1 Vapor Pressure Deficit Formula (McGarigal, 2015)

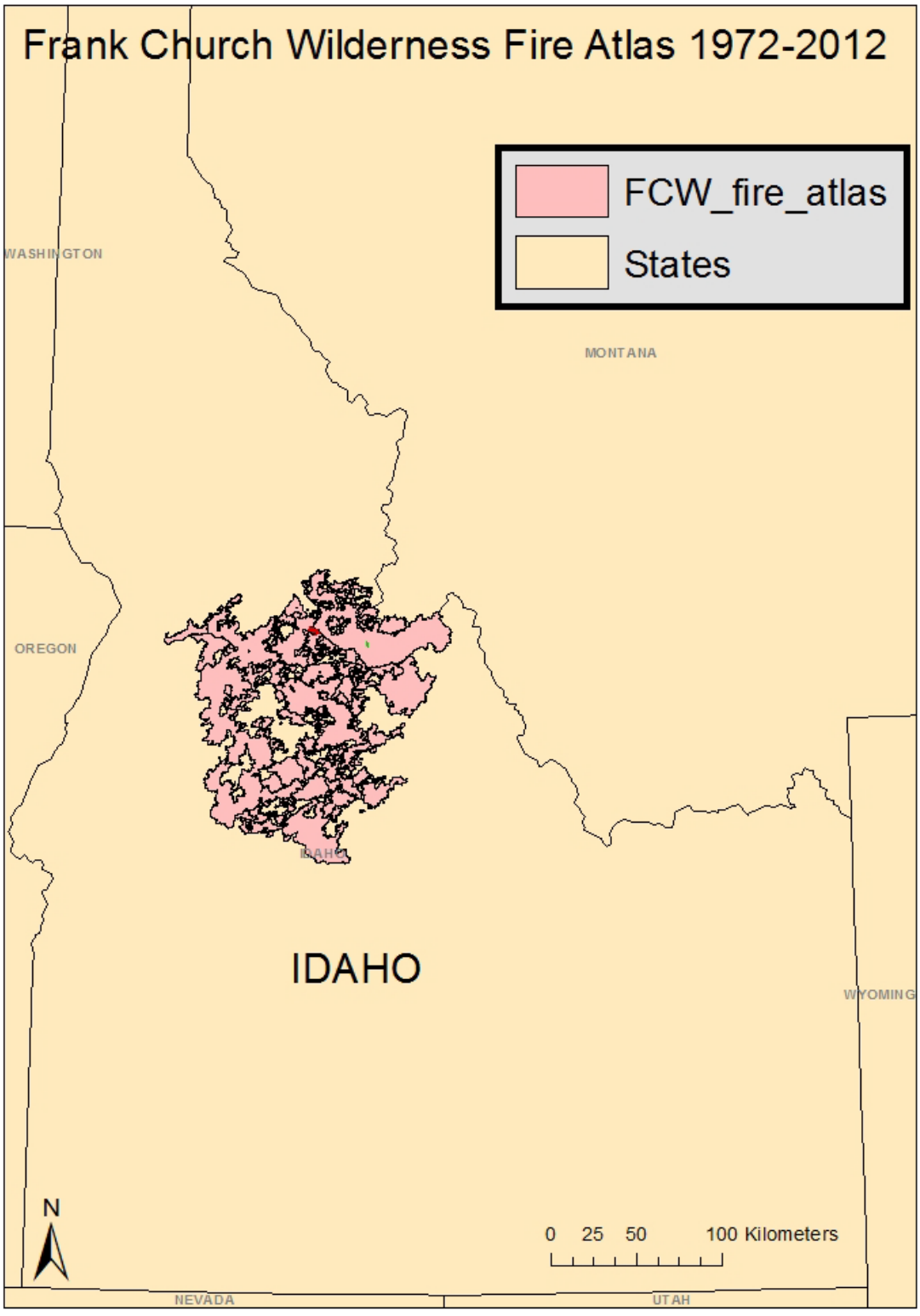

Figure 4. Frank Church Wilderness fire atlas data (from Parks et al., 2015).

Fragstats

I analyzed 290 fires from the fire atlas in FRAGSTATS. There was a loss of seven fires due to edge depths that the software could not identify (i.e., an error in FRAGSTATS was insufficient memory to process).

To answer my research questions, the following climate-related metrics for analysis include VPD, Total Area (TA), Number of Patches (NP), Landscape Shape Index (LSI), and Perimeter-area fractal dimension index (PAFRAC) (see Appendix A). VPD is in units of kPa.

I used a Pearson Correlation Matrix (PCM) to evaluate the metrics. A PCM measures the strength and direction of linear statistical relationships. The requirements to use a PCM include random sampling and continuous data; each variable is independent of one another, one variable must be normally distributed, and all have a linear association and the absence of outliers. I maintained a normal distribution for VPD.

Total Area (TA) is related to climate and equals the total area (m^2) of the landscape, divided by 10,000 (to convert to ha) (Equation 2). All positively valued cells are assumed to be inside the landscape of interest and are included in the total area of the landscape. The TA is related to VPD with a PCM of 0.57, a high positive correlation (see Figure 8; Table 1 and Appendix E).

$$TA = A^*\left(\frac{1}{10{,}000}\right)$$

A - Total landscape area (m^2)

Equation 2 Total Area Formula (McGarigal, 2015)

The Number of Patches (NP) is the total number of patches in the landscape. NP does not include any internal background patches (i.e., within the landscape boundary) or any patches of the landscape border when present. The 8-neighbor rule for delineating patches (and all metrics) was used for this study. NP conveys no information about the patches' area, distribution, or density. However, if the total landscape area is constant, NP gives the same information as patch density or mean patch size as an index.

Table 1. Metrics of Figure 8. including names, units, and range.

Acronym	Name	Units	Range
TA	Total area	hectares	TA > 0, without limit
NP	Number of patches	none	NP > 0, without limit
LSI	Landscape shape index	none	LSI ≥ 1, without limit
PAFRAC	Perimeter-area fractal dimension index	none	1 ≤PAFRAC ≤ 2
VPD	Vapor Pressure Deficit	kPa	VPD > 0, without limit

Landscape Shape Index (LSI) is 0.25 (adjustment for raster format) times the sum of the entire landscape boundary (even if it represents the 'true' edge or not, based on boundary/background choices) and all edge segments (m) within the landscape boundary, including some or all those bordering/backgrounds divided by the square root of the total

landscape area (m^2) (Equation 3). Total landscape area (A) includes the internal background present. LSI provides a standardized measure of the total edge or edge density and adjusts for the size of the landscape. Based on PCM, LSI is related to VPD through 0.48, a solid correlation (see Figure 9).

$$LSI = \frac{0.25 * E}{\sqrt{A}}$$

E - total length (m) of the edge in landscape
(Includes boundary and background edge segments)
A – total landscape area (m^2)

Equation 3 Landscape Shape Index Formula (McGarigal, 2015)

Perimeter-area Fractal Dimension Index (PAFRAC) is the fractal dimension using the perimeter-area method ($A = k P^{2/D}$, where A is the area, k is a constant, P is the perimeter, and the D is a fractal dimension). The fractal dimension is a statistical index of the complexity of a pattern, with higher values indicating more considerable complexity. Imagine approximating a circular shape with a hexagon and a decagon. Hexagon has lower complexity and a lower fractal dimension, whereas decagon is associated with a more complex shape and a larger fractal dimension. PAFRAC's calculation is presented in Equation 4. In rough words, PAFRAC is a shape metric that describes the complexity of patches while independent of their scales. This equation assumes that the area and perimeter of patches are linearly related on a logarithmic scale. This index can have mixed results with small sample size. The sample size is large enough for each fire to not

have mixed results with small samples. In landscapes with only a few patches, it is common to get values that greatly exceed the theoretical limits of this index. This index is mainly helpful in large sample sizes (n > 20). Additional connections were not evaluated through this analysis (see Appendix B).

$$PAFRAC = \frac{2\left[N\sum_{i=1}^{m}*\sum_{j=1}^{n}(ln_{pij} * ln_{aij})\right] - \left[\left(\sum_{i=1}^{m}*\sum_{j=1}^{n}\ln_{pij}\right)\left(\sum_{i=1}^{m}*\sum_{j=1}^{n}\ln_{aij}\right)\right]}{\left(N\sum_{i=1}^{m}*\sum_{j=1}^{n}(\ln_{pij})\,\hat{}\,2\right) - \left(\sum_{i=1}^{m}*\sum_{j=1}^{n}(\ln_{pij})\right)^{2}}$$

a_{ij} - area (m^2) of patch ij
p_{ij} – perimeter (m) of patch ij
N – total number of patches in the landscape

Equation 4 Perimeter-area Fractal Dimension Index Formula (McGarigal, 2015)

RESULTS

An increase in annual burned area from 1972 to 2012 occurred in our study area (see Figure 5, from Landsat imagery by Parks et al., 2015). Note that this plot only shows modern fire patterns.

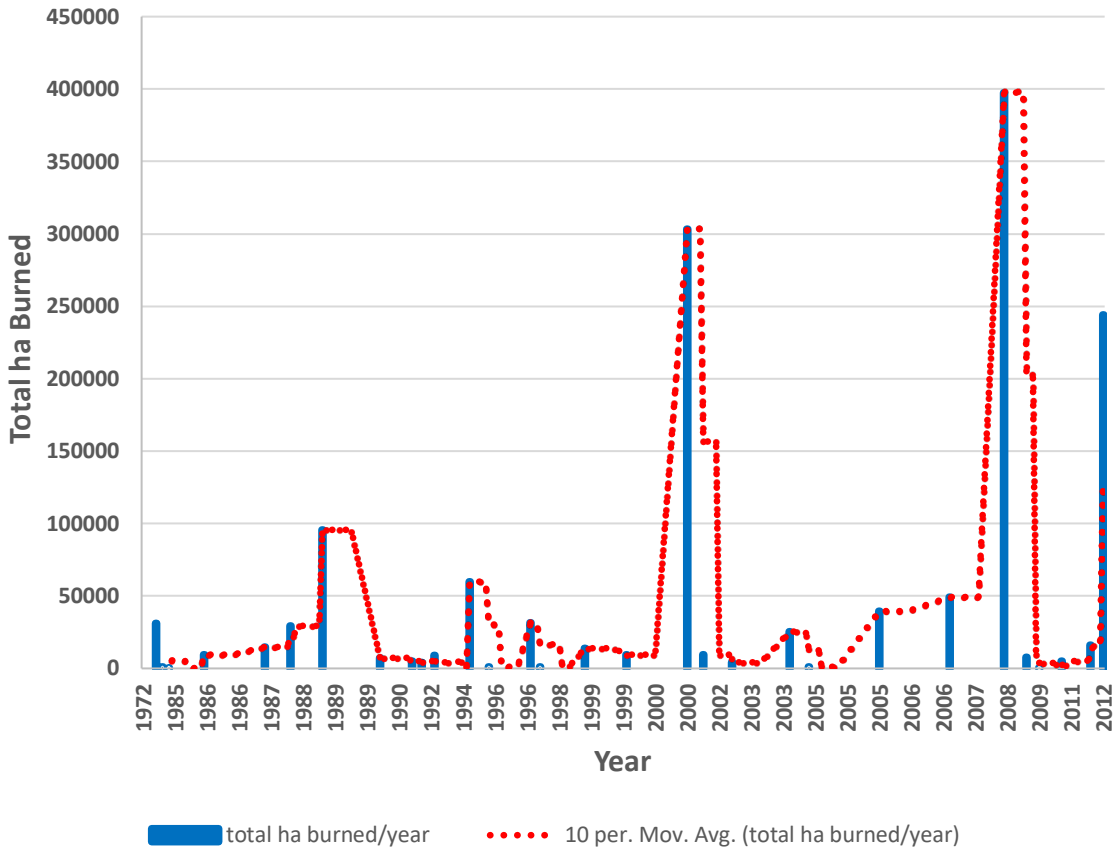

Figure 5. Acres burned in the Frank Church Wilderness study area between 1972-2012. The largest fires were in 1998, 2000, and 2008.

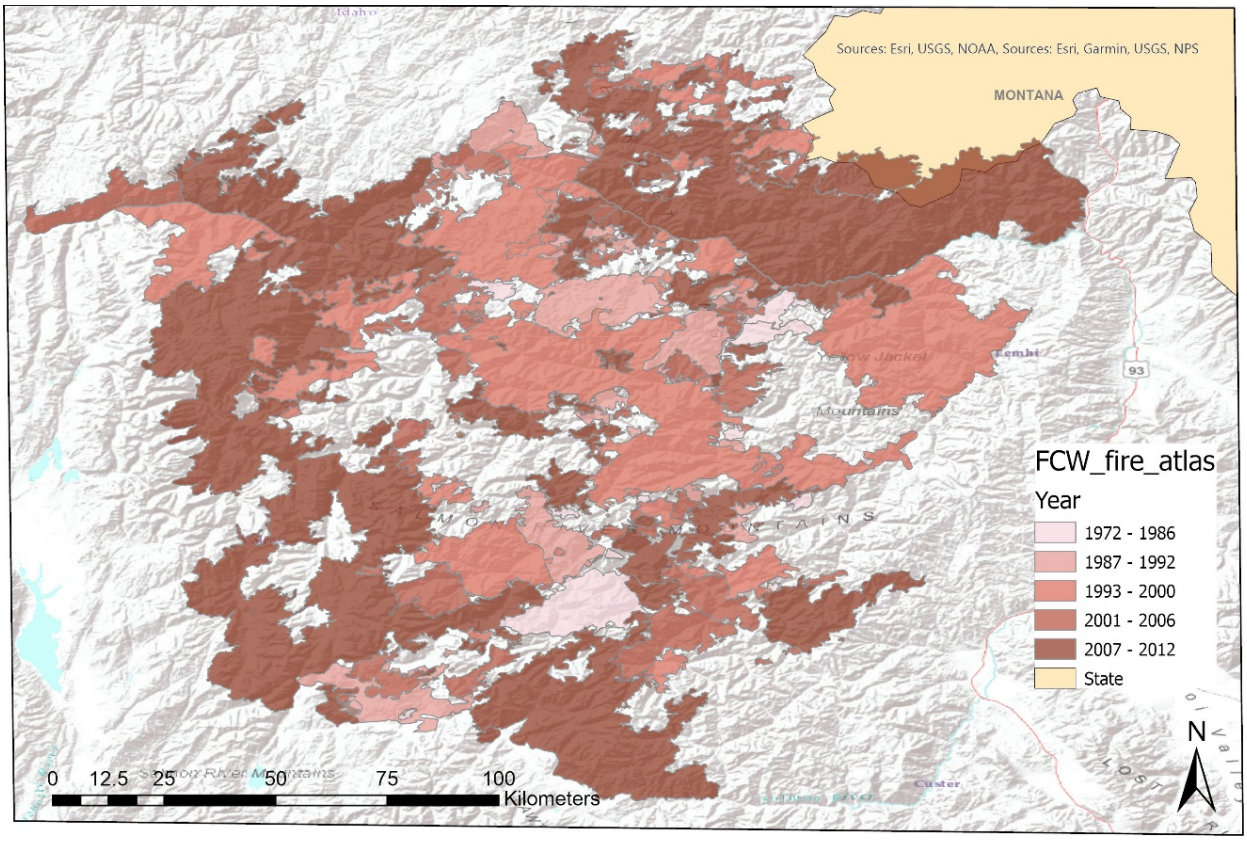

Figure 6. Fire perimeters of the Frank Church wilderness from 1972-2012.

From 1972 to 2012, 284 fires burned 1,326,695 ha in the FCW. Lightning-caused (or naturally started fires) account for most of these fire starts. Records from NIFC (including all of Idaho) show 29 significant fires (over 16,000 ha in size) from 2007-2012 in Idaho 25 (1,200,000 ha) were caused by lightning (8,000 ha), of the fires were started by human ignitions, and 1 (20,000 ha) are of unknown cause. Figure 6 is the fire atlas from the FCW.

Climate Aridity Trends

The linear trend in summer (average of June, July, and August) VPD from 1972-2012 for the study area is shown in Figure 7. The increasing trends in summer VPD translated to a 20% increase in average summer VPD in 2012 compared to 1972.

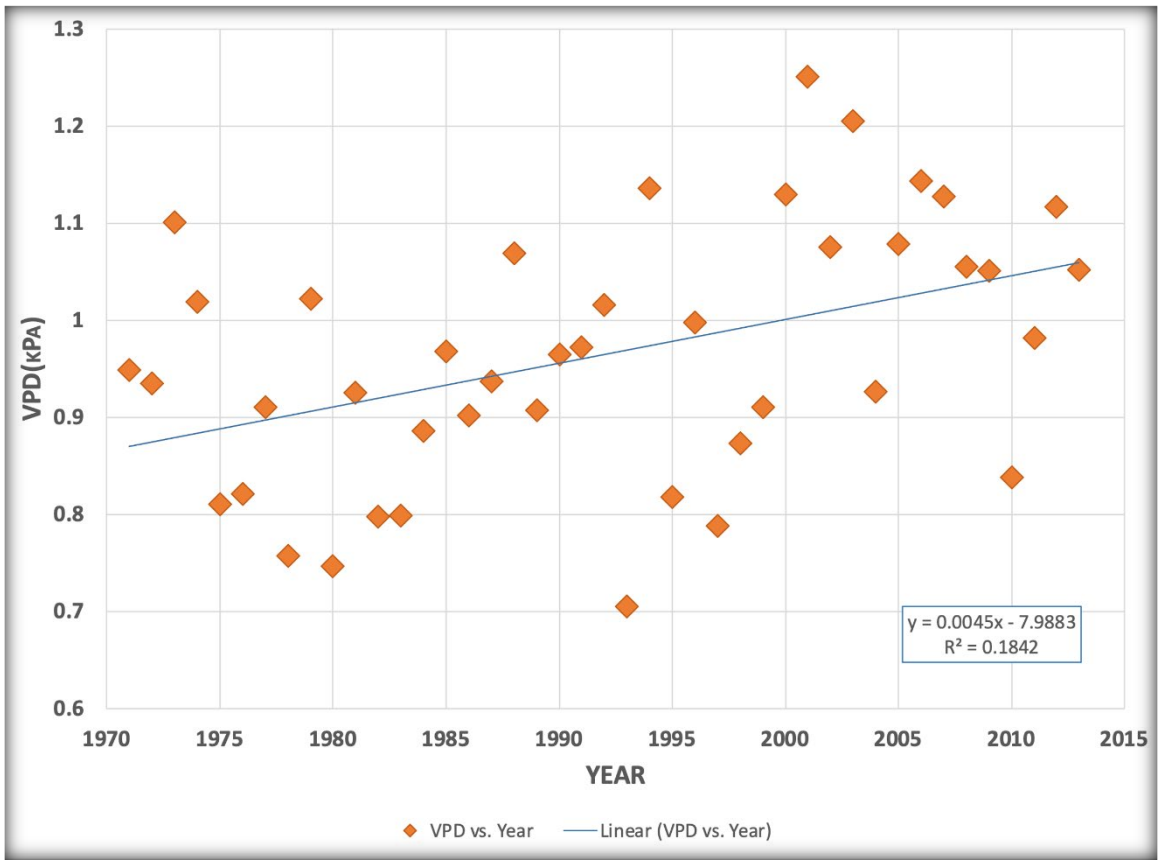

Figure 7. The Vapor Pressure Deficit of the Frank Church Wilderness was collected from the Climate Toolbox (Hegewisch et al., 2022).

Correlation Between Climate Aridity and Landscape Metrics of Burned Area

Figure 8 displays linear relationships between several landscape metrics of burned area derived from FRAGSTATS and summer VPD. Note that this figure shows the landscape metrics with solid linear correlation with summer VPD at the 95% confidence (5% significance) level. The correlation of other landscape metrics with summer VPD was not statistically significant.

Annual burned area (aka total area, TA) and the number of patches of burned area (NP) are logarithmic-exponentially distributed, implying that most fires are small. Only a few large fires generally determine the total burned area in each region, and many fires remain small. Still, those large fires are associated with high socio-environmental consequences. Landscape Shape Index (LSI) and Perimeter Area Fractal Dimension Index (PAFRAC) is skewed toward lower values, and VPD's distribution is bell-shaped. Based on PCM, PAFRAC relates to VPD with a -0.37 (negative) correlation. LSI is the ratio between the actual landscape edge length and the hypothetical minimum edge length. Higher LSI is associated with more patches. PAFRAC measures the complexity of the edges of each burned patch. For example, hexagon edges are more complex than the edges of a circle. The distribution of LSI and PAFRAC shows that most burned patches are not too complicated in shape. However, they are not too simple either. Note that 30-m Landsat resolution also influences the complexity of the edges of burned patches. Summer VPD distribution shows that most years are in a medium VPD level, although low VPD (cold-wet) and high VPD (very hot-dry) are also present. This distribution skews toward higher VPD values as the climate warms (see Figure 7).

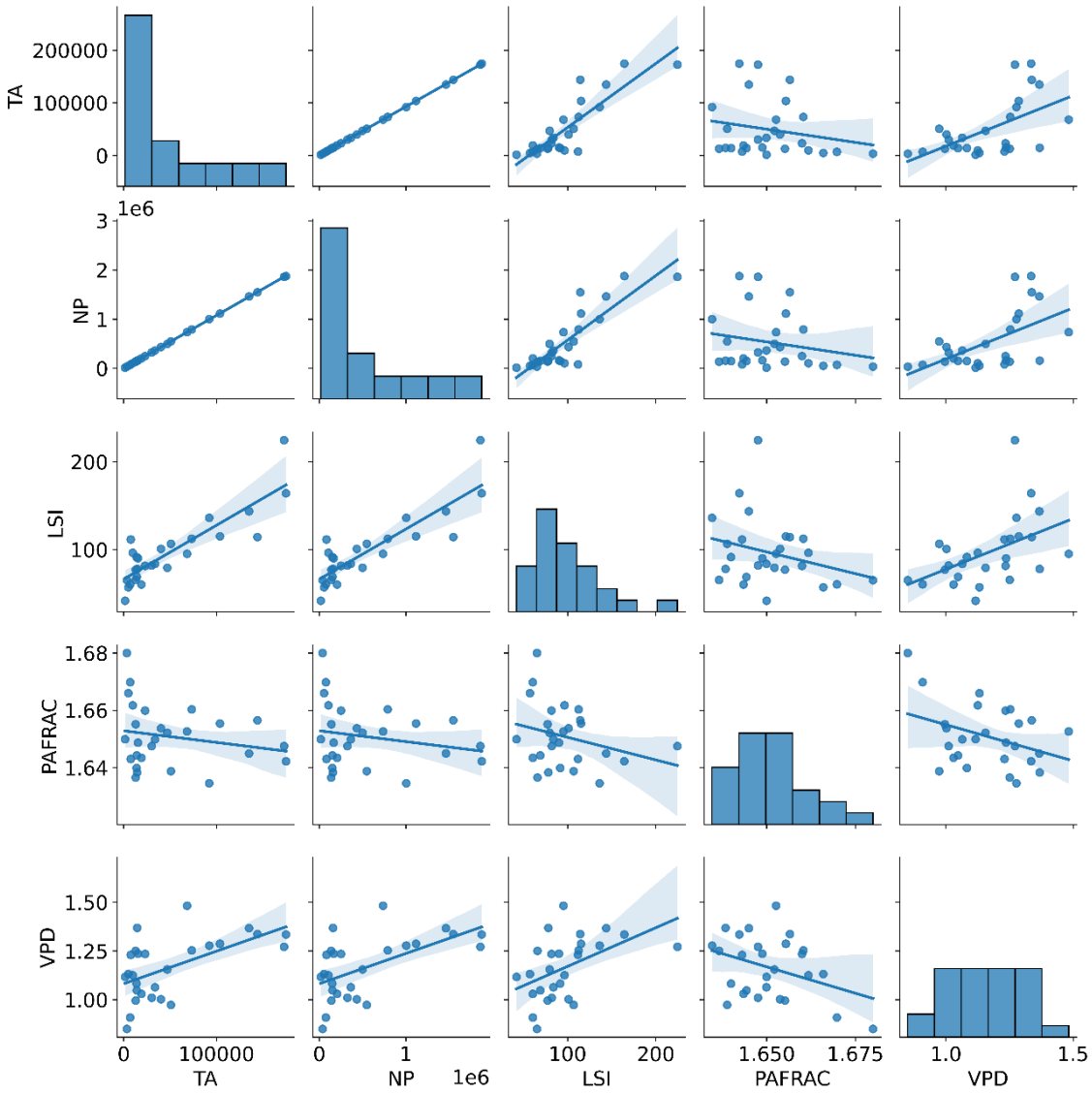

Figure 8. Python constructed vapor pressure deficit correlation to FRAGSTATS metrics. VPD data is from the climate toolbox, and other data is derived from FRAGSTATS calculation.

Bivariate relationships between landscape metrics of burned area and summer VPD.

First and foremost, annual burned area is highly correlated with summer VPD, with a Pearson correlation coefficient of 0.57 and a p-value of 0.002. A positive correlation indicates that an increase in summer VPD generally translates to a higher annual burned area, implying that a warmer and drier future is associated with an increasing burned area. A closer look at the bivariate scatter plot of VPD-TA reveals exciting findings. Expectedly, all "high" annual burned areas occurred at "high" summer VPD years (at the top right quarter of the VPD-TA plot). However, low annual burned areas occurred during high and low summer VPD years. The highest summer VPD is not associated with the highest annual burned area (mid plot in VPD-TA), and several high summer VPDs are associated with the low annual burned area. Several reasons underpin such behavior. Here, I am using summer VPD, and many large fires grow on days with extreme fire-weather characteristics (dry-hot-windy). The mismatch between the temporal scale of VPD and fire growth can explain some of the observed VPD-TA relationships. Also, note that fires are stochastic processes, and treating them as deterministic, as done in Figure 8, can introduce errors. Furthermore, fire characteristics are governed by many other variables not captured in VPD, including fuel availability and connectivity, wind, and topography, among others. A similar observation is also made for the VPD-NP (number of patches) relationship.

Landscape Shape Index (LSI) and summer VPD correlate positively with a Pearson correlation coefficient of 0.48 and a p-value of 0.01. While this relationship is complex and depends on other factors such as topography and fuel availability, higher

VPD values (hotter and drier climate) are expected to enable more concentrated burn patches (uniform burn through the landscape), which is associated with a lower LSI. However, a positive VPD-LSI relationship implies higher VPD is associated with a less uniform burn. There might be two hypotheses that can explain this, which require more analysis and are beyond the scope of this study. First, a significant portion of the observed high correlation is due to a single high LSI value (see Figure 9, VPD-LSI plot), and if that point is removed, the correlation value will change. The second hypothesis is that high VPD years can be conducive to more spotting fires, meaning that fuel is hotter and drier, wind can transport ambers to longer distances, and fuels are receptive to ignition by ambers. So, fires not only expand by convective processes but also by ambers and several patches that burn throughout one fire. This is indeed an exciting research question for follow-up studies.

On the other hand, the Perimeter Area Fractal Dimension Index (PAFRAC) is negatively correlated with summer VPD, indicating that hotter and drier summers are associated with less fractal dimension. This implies that hotter and drier summers are conducive to more uniform burns on the edges of patches, meaning everything will burn, and there is less wiggle on the outer edges of fire patches. Summer VPD and PAFRAC have a Pearson correlation coefficient of -0.38 and a p-value of 0.05.

Correlation Between Various Landscape Metrics of Burned Area

Total annual burned area and number of patches (TA-NP in Figure 8) are significantly correlated (at a significance level of 0.001) with a Pearson correlation coefficient of almost one. This intuitive relationship shows that as the number of burned patches increases, so does the total burned area and vice versa. An implicit implication of

this finding is that increasing burned area does not necessarily happen within larger connected patches however happens with more patches being burned. Assuming that this finding is not an artifact of satellite imagery processing and post-processing of burned area imagery in FRAGSTATS, this observation also confirms our previous hypothesis that a fire spot is a significant way of fire propagation in the study area.

Landscape Shape Index (LSI) and annual burned area (TA), and the number of burned patches (NP) are also positively and significantly correlated, with a Pearson correlation coefficient of 0.86 and with a p-value of less than 0.001 (Figure 8). This is somewhat expected as higher patchiness is associated with higher LSI. This relationship would have been reversed if fires were to burn in one sizeable circular patch. Still, since fires in the study area are burning in many patches (given previously stated assumptions), this LSI-TA and LSI-NP correlation are positive and significant.

Perimeter Area Fractal Dimension Index (PAFRAC) and annual burned area (TA), and the number of burned patches (NP) showed a negative but non-significant correlation (Pearson correlation coefficient of -0.2, statistically not significant; Figure 8). This indicates that burned area edges are generally less fragmented as fires grow larger. However, this relationship can be merely due to the randomness of the data, given this relationship is not statistically significant. Similarly, PAFRAC and LSI are negatively correlated (Pearson correlation coefficient of -0.38), but this correlation is not statistically significant.

DISCUSSION

Fires in Idaho and across western North America are increasing, and it is essential to study them as more people, and natural habitats become at risk of wildfires. Wildfire records are available in open-source options, and this will help the public and scientists communicate with common terminology to improve the understanding of wildfires. Climate and landscape metrics in the Frank Church Wilderness (FCW) are accessible and understanding the landscape through vegetation components is valuable.

Fire in Idaho

According to NIFC, in 2021, Idaho had 1,332 fires, 177,900 ha. In the three significant fires in 2021, over 40,000 (98,000 ha burned total) were lightning caused. Idaho made the top five in the nation for extreme wildfire risks according to FireLine® (Verisk, 2021). Verisk's wildfire risk management tool calculated 175,000 properties at risk of wildfire. In total, 26% of properties in Idaho are at risk for wildfire damage.

Understanding the FCW's fire regime is key to understanding the response to climate and landscape change in a wilderness area that has been unmanaged. In 2016, the USDA evaluated a typical fire return interval for high elevation mixed conifer forests in the Northern Rocky Mountains. The USDA estimated warm and dry ponderosa pine forests had mean fire-return intervals of 10 to 25 years (n = 137 plots) from about 1900 to 1935 (Fryer, 2016). In dry ponderosa pine -Douglas-fir forests, the stands had both frequent and not frequent surface fires and moderate-interval, moderate-severity fires, with mean fire-return intervals ranging from 20 to 40 years (n = 117 plots) (Fryer, 2016).

Before fire exclusion began in the FCW in the early 1930s, fires in ponderosa pine communities were frequent inside and outside the FCW (Fryer, 2016). The trees sampled inside the FCW had fewer fire scars than outside (Fryer, 2016).

Climate and Vegetation in the Frank Church Wilderness

Using VPD from May through September annually provides a critical seasonal moisture representation of climate. Fuel continuity and moisture are the main limiting factors of burnt areas globally (Kelley et al., 2019). Vegetation in the form of fuel is shaped by location, temperature, and elevation, with future predictions of climate-driven changes (IPPC, 2022). Rehfeldt et al. (1999) evaluated data that showed small climate changes would significantly affect tree populations' growth and survival.

Implications for Future Work

Creating and evaluating the FRAGSTATS metrics provide additional available data for comparison and further investigation of wildfire changes in central Idaho. This study can be used in future studies to compare wildfire changes in unmanaged wildernesses with adjacent managed forests to examine if and how prior management (fire suppression, logging, etcetera) influenced fires in high elevation mixed conifer forests. The FCW is large, and the need to compare an equally large area that has been heavily managed could be a future project. An ideal comparative location for the prospective study is the national forests surrounding the FCW, which have a long history of logging, fire suppression, and other management activity.

Limitations

A fire's size can generate limitations for evaluation in that evolution of a natural fire regime can be reduced by previous burning (Haire et al., 2013). The research range is a limitation identified by Burnicki (2012). Like this study, the pattern analysis of maps shows landscape metrics individually, which significantly impacts the overall results. It is necessary to understand the complex nature of natural processes and their relationship to fire regimes. The extensive fire data that Parks et al. (2015) collected is valuable in understanding the considerable fire complexity of The Frank Church Wilderness. A limitation of usable satellite imagery is a common challenge with remote sensing (Fornacca et al., 2020).

CONCLUSION

Through this study, I investigated the control of vapor pressure deficit (VPD; i.e., climate aridity) on landscape metrics of burned area (using the FRAGSTATS software) in the Frank Church Wilderness from 1972-2012. The relationship between climate and VPD was compared to the FRAGSTATS metrics total area, the number of patches, landscape shape index, and perimeter-area fractal dimension index. VPD and specific landscape metrics associated with burned areas were highly correlated. This relationship indicates that a fire's burned area correlates directly to climate aridity.

A Pearson Correlation Matrix (PCM) is essential in measuring the strength and existence of a linear relationship between two variables, and if the outcome is significant, a correlation exists. AA PCM of our data is available in Appendix E and a supplemental Excel file. TA relates to VPD through the total landscape of the area and has a strong positive correlation. NP relates to VPD through the density of the patch size unrelated to an area (TA is related to the area) with just as significant a high correlation as TA. LSI relates to VPD from the corrections made to spatial edge density and area distribution on the landscape; after the modifications, it has a strong correlation. PAFRAC relates to VPD by having a negative correlation; this means when all patches are considered in the landscape, it becomes negatively connected to VPD (as VPD increases, PAFRAC decreases).

Many FRAGSTATS metrics were correlated, and some had dependencies that showed significance in describing a fire distribution change in the landscape. The

FRAGSTATS metrics were chosen through connection to climate and how they relate to one another. This provided insight into what metrics are worth using for future studies. The landscape metric process, statistical evaluation from our FRAGSTATS methods, and the collection of VPD data from the Climate Toolbox can be reproduced. This allows a comparison to neighboring wildernesses or forested areas beyond this study.

A powerful choice is using open-source software such as FRAGSTATS to promote accessibility in science. For this reason, I wanted to ensure the scientific community would have access to the study to be able to replicate and continue this research. The available software and data allow more scientists and community members to explore wildfires in this study.

REFERENCES

Alizadeh, M.R., Abatzoglou, J.T., Luce, C.H., Adamowski, J.F., Farid, A. and Sadegh, M., 2021. Warming enabled upslope advance in western US forest fires. Proceedings of the National Academy of Sciences, 118(22).

Burnicki, A. C. (2012). Impact of an error on landscape pattern analyses performed on land-cover change maps. Landscape Ecology, 27(5), 713-729.

EDW, USDA. EDW_RAVG_01. (2019, March 15). Published raw data. (EDW/EDW_RAVG_01 (MapServer) (usda.gov)).

Fornacca, D., Ren, G. and Xiao, W., 2020. Small fires, frequent clouds, rugged terrain, and no training data: a methodology to reconstruct fire history in complex landscapes. International Journal of Wildland Fire, 30(2), pp.125-138.

Fryer, Janet L. 2016. Fire regimes of Northern Rocky Mountain ponderosa pine communities. In: Fire Effects Information System, [Online]. U.S. Department of Agriculture, Forest Service, Rocky Mountain Research Station, Missoula Fire Sciences Laboratory (Producer). Available: www.fs.fed.us/database/feis/fire_regimes/Northern_RM_ponderosa_pine/all.html [May 11, 2021].

Gergel, S. E., & Turner, M. G. (Eds.). (2017). Learning landscape ecology: a practical guide to concepts and techniques. Springer

Haire, S.L., McGarigal, K. and Miller, C., 2013. Wilderness shapes contemporary fire size distributions across landscapes of the western United States. Ecosphere, 4(1), pp.1-20.

Hegewisch, K.C., Laquindanum, V., Fleishman, E., Hartmann, H., and Mills-Novoa, M.. Climate Toolbox Tool Summary series. https://ClimateToolbox.org. [January 28, 2022].

Heyerdahl, E.K., Morgan, P. and Riser, J.P., 2008. Multi-season climate synchronized historical fires in dry forests (1650–1900), northern Rockies, USA. Ecology, 89(3), pp.705-716.

Heyerdahl, E. K., Loehman, R. A., & Falk, D. A. (2019). A multi-century history of fire regimes along a transect of mixed-conifer forests in central Oregon, USA. Canadian Journal of Forest Research, 49(1), 76-86.

Higuera, P.E. and Abatzoglou, J.T., 2020. Record-setting climate enabled the extraordinary 2020 fire season in the western United States. Global change biology, 27(1), pp.1-2.

IPCC, 2022: Climate Change 2022: Impacts, Adaptation, and Vulnerability. Contribution of Working Group II to the Sixth Assessment Report of the Intergovernmental Panel on Climate Change [H.-O. Pörtner, D.C. Roberts, M. Tignor, E.S. Poloczanska, K. Mintenbeck, A. Alegría, M. Craig, S. Langsdorf, S. Löschke, V. Möller, A. Okem, B. Rama (eds.)]. Cambridge University Press. In Press.

Kelley, Douglas I., et al. "How contemporary bioclimatic and human controls change global fire regimes." Nature Climate Change 9.9 (2019): 690-696

Krawchuk, M.A., Moritz, M.A., Parisien, M.A., Van Dorn, J. and Hayhoe, K., 2009. Global pyrogeography: the current and future distribution of wildfire. PloS one, 4(4), p.e5102.

Levin, S. A. (1976). Spatial patterning and the structure of ecological communities. Some mathematical questions in biology, 7, 1-35.

McCaffrey, S., McGee, T. K., Coughlan, M., & Tedim, F. (2020). Understanding wildfire mitigation and preparedness in the context of extreme wildfires and disasters: Social science contributions to understanding human response to wildfire. Extreme Wildfire Events and Disasters: Root Causes and New Management Strategies, 155–174. https://doi.org/10.1016/B978-0-12-815721-3.00008-4

McGarigal, K., 2015. FRAGSTATS help. University of Massachusetts: Amherst, MA, USA, p.182.

Morgan, P., Heyerdahl, E.K., Miller, C., Wilson, A.M. and Gibson, C.E., 2014. Northern Rockies pyrogeography: an example of fire atlas utility. Fire Ecology, 10(1), pp.14-30.

NASA. (n.d.). California continues to burn. NASA. Retrieved October 11, 2020, from https://earthobservatory.nasa.gov/images/147215/california-continues-to-burn

NIFC. (n.d.). National Report of wildland fires and acres burned by State. https://www.predictiveservices.nifc.gov/intelligence/2020_statssumm/fires_acres20.pdf Accessed 2021-05-11.

Ostapowicz, K., Vogt, P., Riitters, K. H., Kozak, J., & Estreguil, C. (2008). Impact of scale on morphological spatial pattern of forest. Landscape ecology, 23(9), 1107-1117.

Parks, Sean A.; Holsinger, Lisa M.; Miller, Carol; Nelson, Cara R.. (2015). Fire atlas for the Frank Church-River of No Return Wilderness. Forest Service Research Data Archive. https://doi.org/10.2737/RDS-2015-0021. Accessed 2021-04-15.

Parks, S. A., Holsinger, L. M., Miller, C., & Parisien, M. A. (2018). Analog-based fire regime and vegetation shifts in mountainous regions of the western US. Ecography, 41(6), 910-921.

Rehfeldt, G. E., Ying, C. C., Spittlehouse, D. L., & Hamilton Jr, D. A. (1999). Genetic responses to climate in Pinus contorta: niche breadth, climate change, and reforestation. Ecological monographs, 69(3), 375-407.

Rollins, M.G., Swetnam, T.W. and Morgan, P., 2001. Evaluating a century of fire patterns in two Rocky Mountain wilderness areas using digital fire atlases. Canadian Journal of Forest Research, 31(12), pp.2107-2123.

Singleton, M.P., Thode, A.E., Sánchez Meador, A.J., Iniguez, J.M. and Stevens, J.T., 2021. Management strategy influences landscape patterns of high-severity burn patches in the southwestern United States. Landscape Ecology, 36(12), pp.3429-3449.

USDA. Fire Effects Information System (FEIS), Northern Rocky Mountain ponderosa pine. (n.d.)., 2016. Retrieved May 25, 2022, from https://www.fs.fed.us/database/feis/fire_regimes/Northern_RM_ponderosa_pine/all.html

USDA. (2021). Frank Church-River of No Return Wilderness. Nez Perce-Clearwater National Forests - Frank Church-River of No Return Wilderness. Retrieved April 20, 2021, from https://www.fs.usda.gov/recarea/nezperceclearwater/recarea/?recid=16476

USDA. (2022). Frank Church River of No Return Wilderness. Forest Service National Website. Retrieved July 28, 2022, from https://www.fs.usda.gov/recarea/payette/recreation/picnickinginfo/recarea/?recid=82965&actid=70

Westerling, A.L., Hidalgo, H.G., Cayan, D.R. and Swetnam, T.W., 2006. Warming and earlier spring increase western US forest wildfire activity. Science, 313(5789), pp.940-943.

2021 Verisk Wildfire Risk Analysis. Verisk. (n.d.). Retrieved May 25, 2021, from https://www.verisk.com/insurance/campaigns/location-fireline-state-risk-report/#:~:text=Verisk%20Wildfire%20Risk%20Analysis%20uses%20data%20from%20FireLine,contributing%20to%20wildfire%20risk%E2%80%94fuel%2C%20slope%2C%20and%20road%20access.

2022 Earth Stripes. (n.d.). Idaho - Climate Change. Earth Stripes. Retrieved June 1, 2022, from https://www.earthstripes.org/result/?country=US&state=ID

APPENDIX A

Metrics for Fire Analysis in FRAGSTATS

Table 2. The metrics calculated in FRAGSTATS are adapted from (McGarigal, 2015 and Singleton et al., 2021).

Acronym	Name	Units	Range
NP	Number of patches	none	NP > 0, without limit
PD	Patch density	number per 100 hectares	PD > 0, without limit
LPI	Largest patch index	percent	0 < LPI ≤ 100
ED	Edge density	m/ha	ED ≥ 0, without limit
AREA_MN	Mean patch size	hectares	AREA > 0, without limit
AREA_AM	Area-weighted mean patch size	hectares	AREA > 0, without limit
AREA_CV	Patch size coefficient of variation	hectares	AREA > 0, without limit
GYRATE_MN	Mean radius of gyration	meters	GYRATE ≥ 0, without limit
GYRATE_AM	Area-weighted mean radius of gyration	meters	GYRATE ≥ 0, without limit
GYRATE_CV	Radius of gyration coefficient of variation	meters	GYRATE ≥ 0, without limit
LSI	Landscape shape index	none	LSI ≥ 1, without limit

COHESION	Patch cohesion index	none	0 < COHESION < 100
SHAPE_MN	Mean shape index	none	SHAPE ≥ 1, without limit
AI	Aggregation index	percent	0 ≤ AI ≤ 100
SHAPE_CV	Shape index coefficient of variation	none	SHAPE ≥ 1, without limit
FRAC_MN	Mean fractal dimension	none	1 ≤ FRAC ≤ 2
FRAC_AM	Area-weighted mean fractal dimension	none	1 ≤ FRAC ≤ 2
FRAC_CV	Fractal dimension coefficient of variation	none	1 ≤ FRAC ≤ 2
PARA_MN	Mean perimeter-area ratio	none	PARA > 0, without limit
PARA_AM	Area-weighted mean perimeter-area ratio	none	PARA > 0, without limit
PARA_CV	Perimeter-area ratio coefficient of variation	none	PARA > 0, without limit

CONTIG_MN	Mean contiguity index	none	0 ≤ CONTIG ≤ 1
CONTIG_AM	Area-weighted mean contiguity index	none	0 ≤ CONTIG ≤ 1
CONTIG_CV	Contiguity index coefficient of variation	none	0 ≤ CONTIG ≤ 1
PLADJ	Percentage of like adjacencies	percent	0 ≤ PLADJ ≤ 100
IJI	Interspersion and juxtaposition index	percent	0 < IJI ≤ 100
SHEI	Shannon's Evenness index	none	0 ≤SHEI ≤ 1
PAFRAC	Perimeter-area fractal dimension index	none	1 ≤PAFRAC ≤ 2
CONTAG	Contagion index	percent	0 <CONTAG ≤ 100
TA	Total area	hectares	TA > 0, without limit

APPENDIX B

Excel Sensitivity Analysis

Additional not evaluated metric connections from Excel 2-19-22

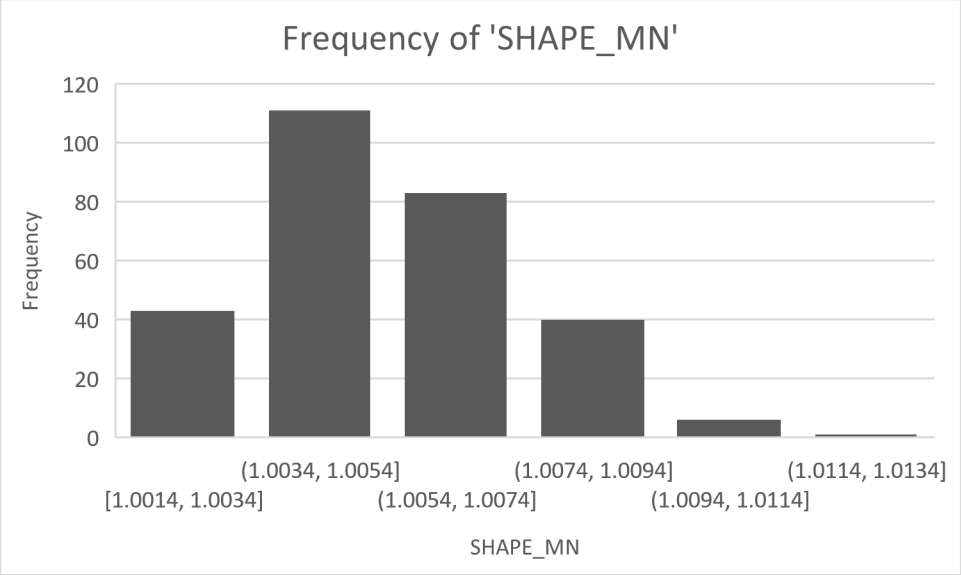

Figure B-1. Frequency of Shape_MN

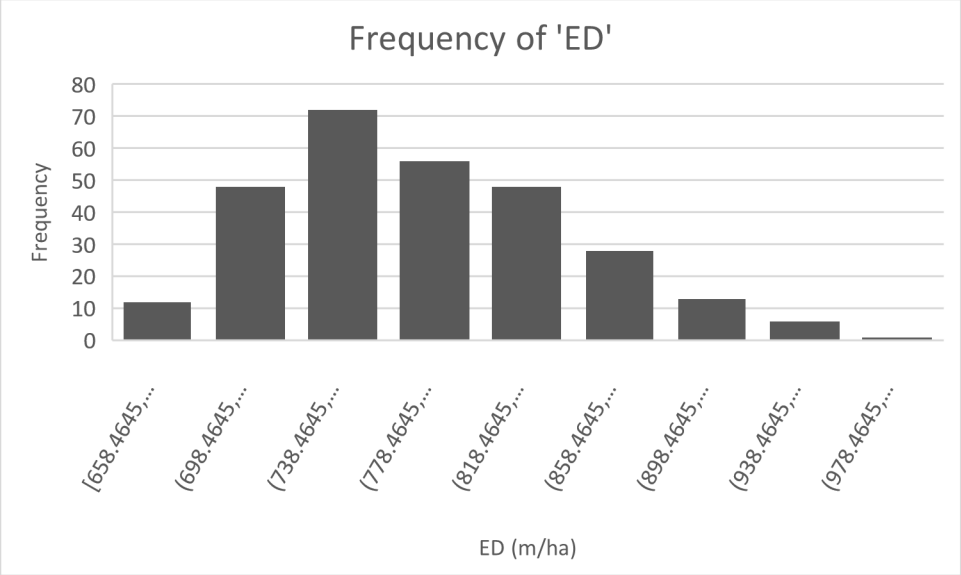

Figure B-2. Frequency of ED

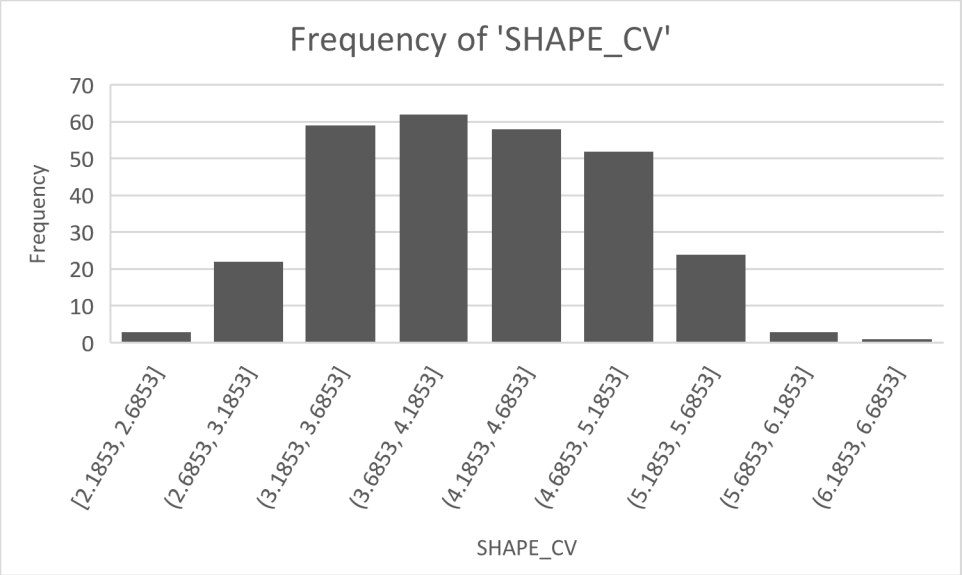

Figure B-3. Frequency of Shape_CV

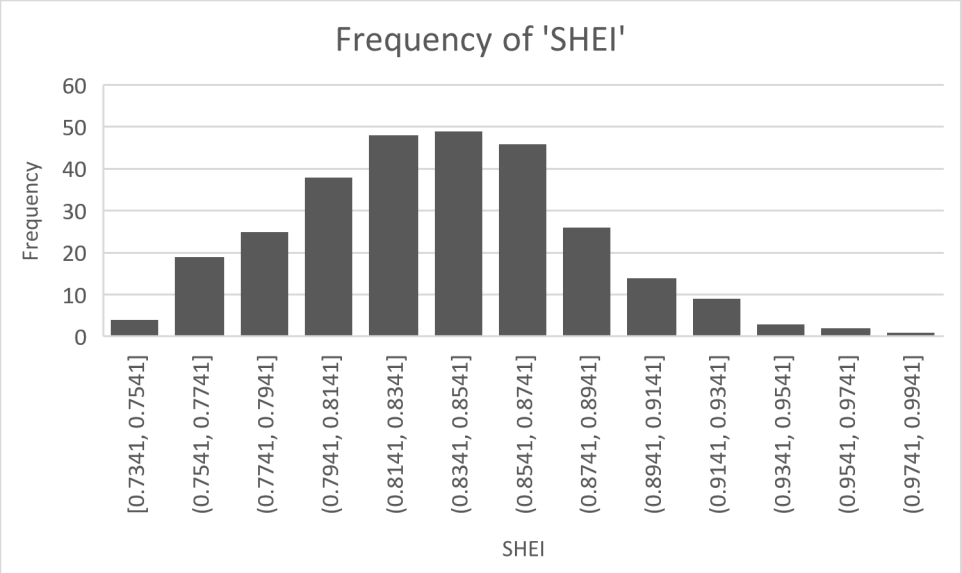

Figure B-4. Frequency of SHEI

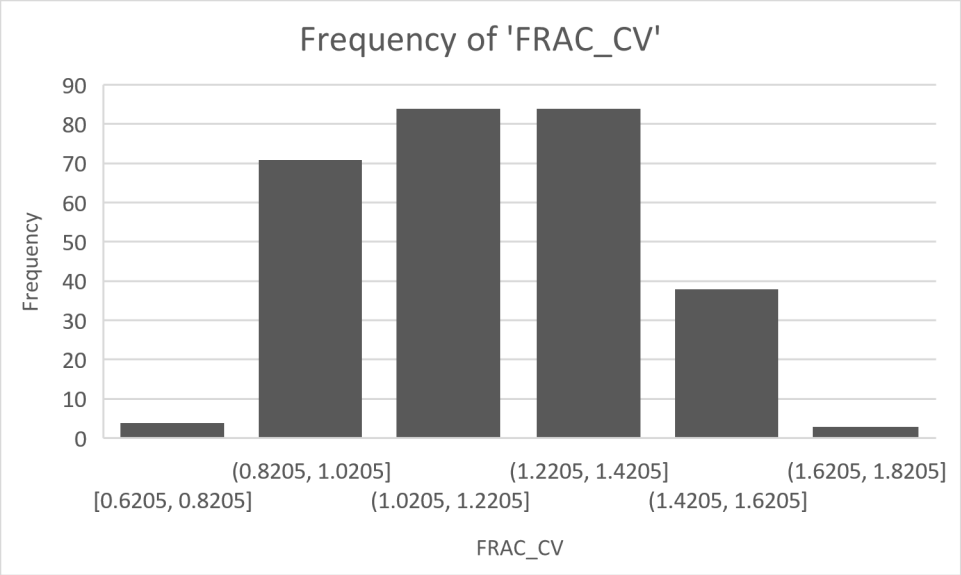

Figure B-5. Frequency of FRAC_CV

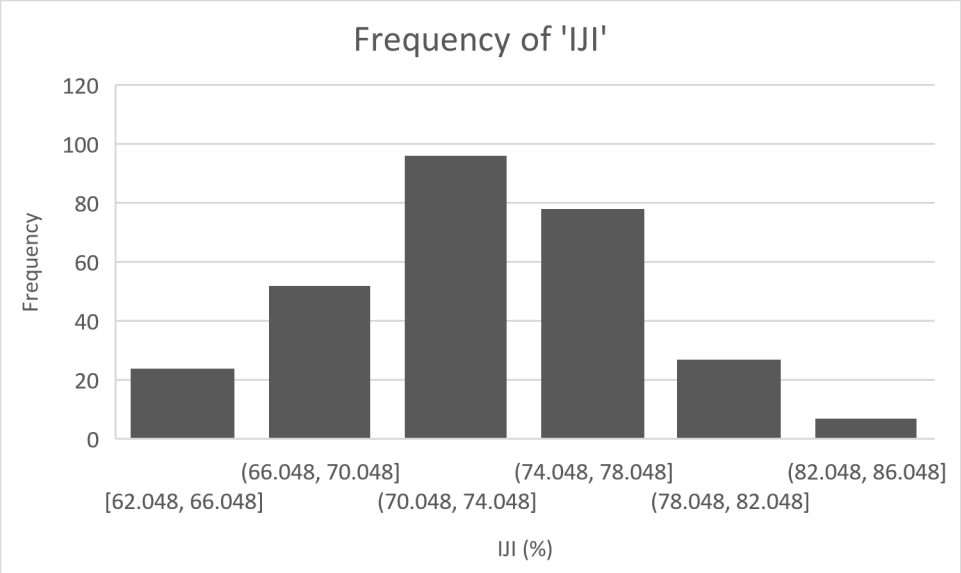

Figure B-6. Frequency of IJI

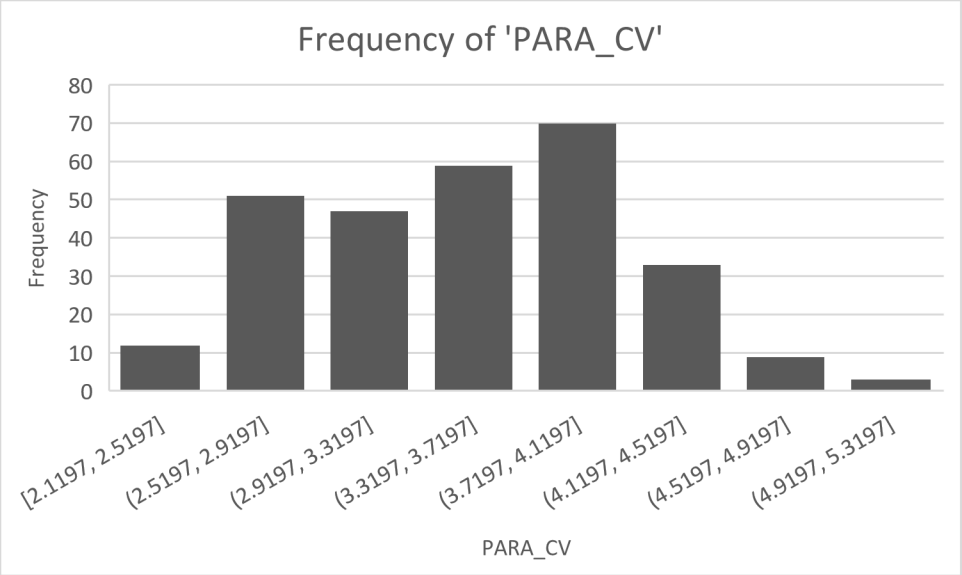

Figure B-7. Frequency of PARA_CV

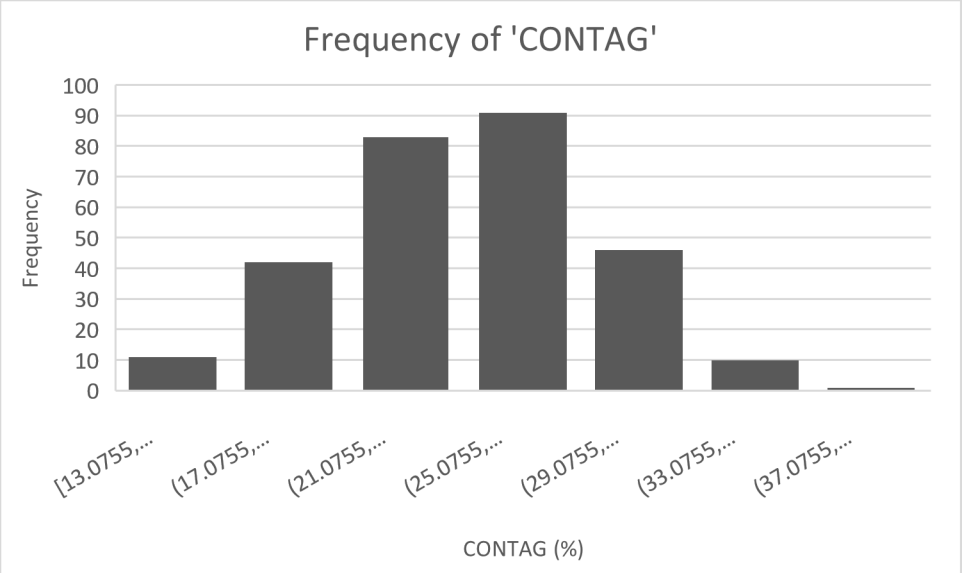

Figure B-8. Frequency of CONTAG

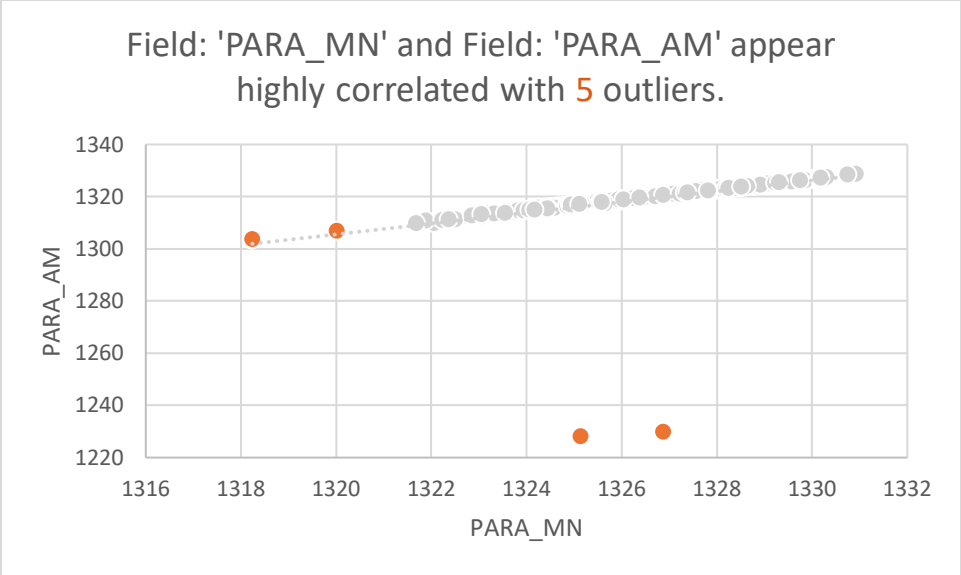

Figure B-9. High Correlation of PARA_MN and PARA_AM

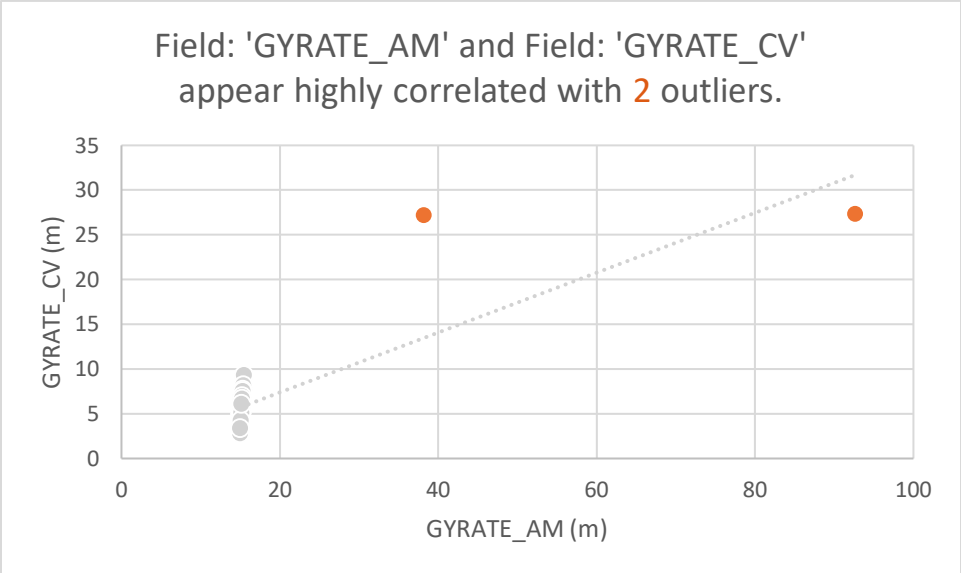

Figure B-10. High Correlation of GYRATE_AM and GYRATE_CV

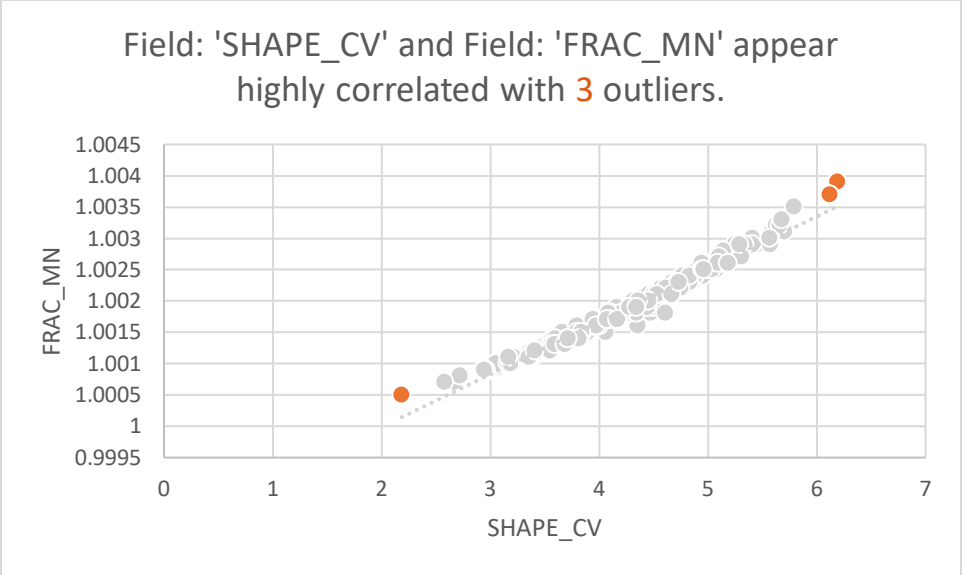

Figure B-11. High Correlation of SHAPE_CV and FRAC_MN

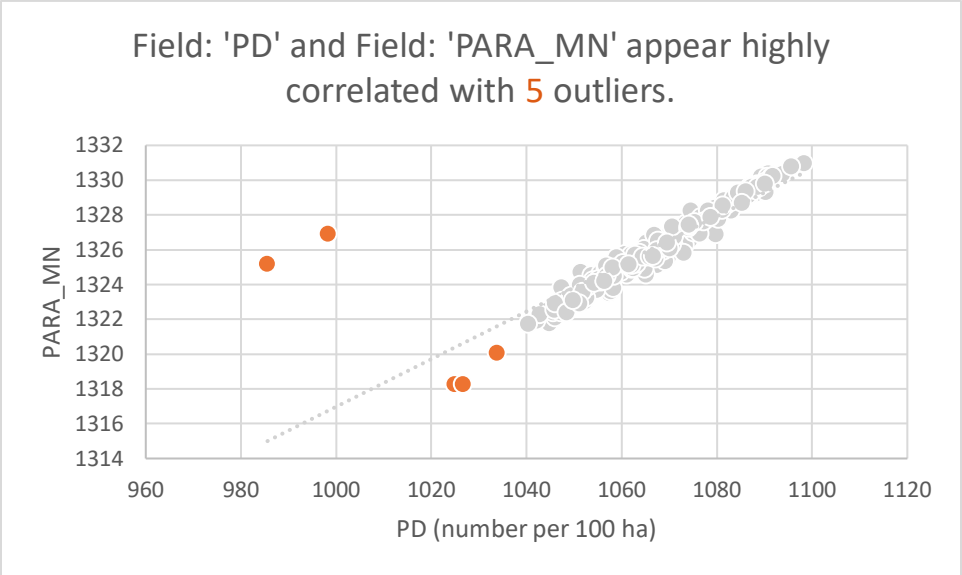

Figure B-12. High Correlation of PD and PARA_MN

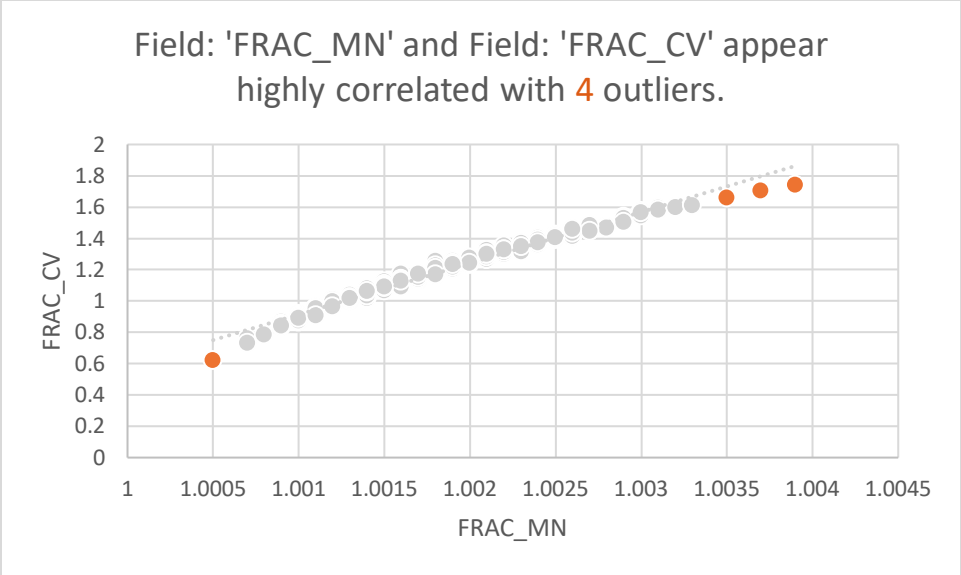

Figure B-13. High Correlation of FRAC_MN and FRAC_CV

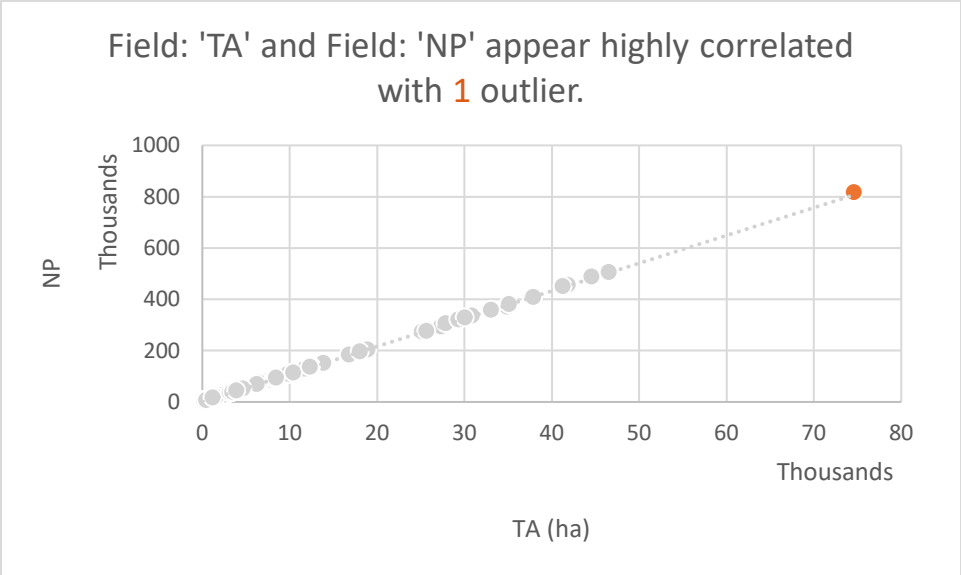

Figure B-14. High Correlation of TA and NP

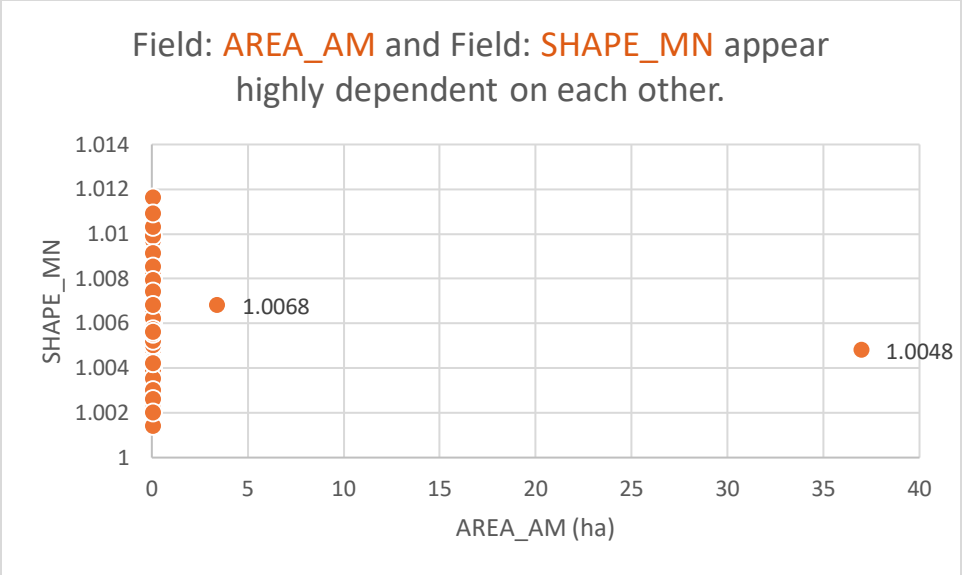

Figure B-15. Highly Dependent between AREA_CV and SHAPE_MN with a PCM value at 0.99

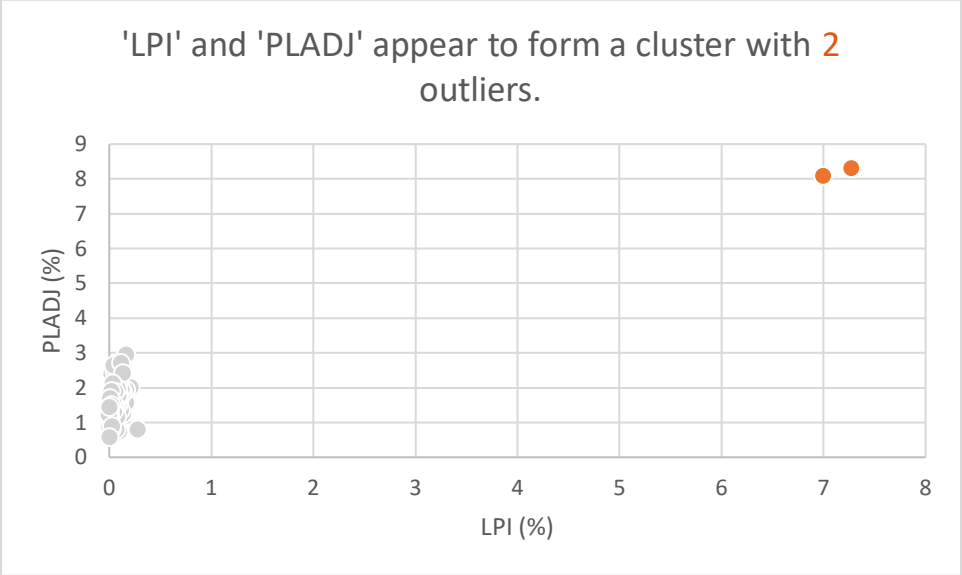

Figure B-16. Cluster between LPI and PLADJ

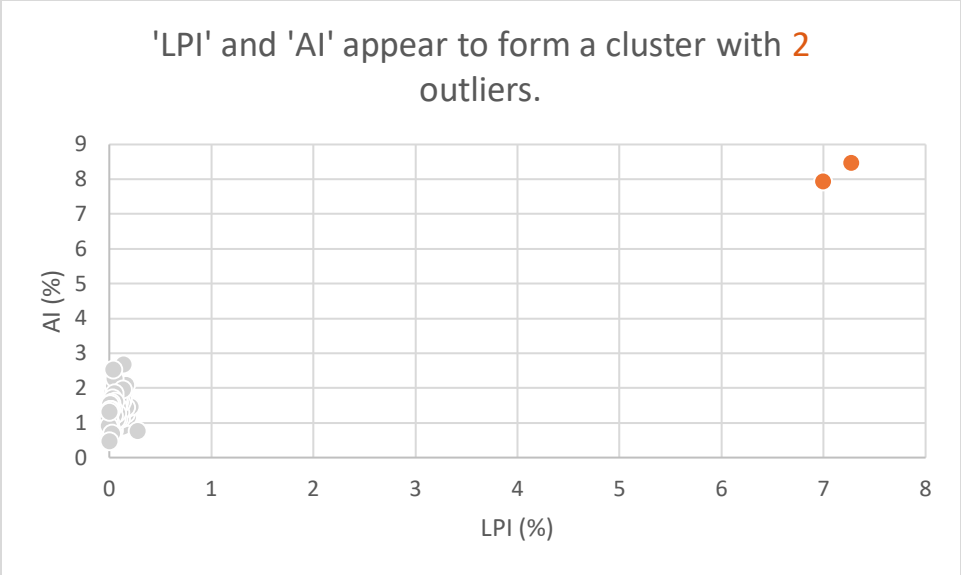

Figure B-17. Cluster between LPI and AI

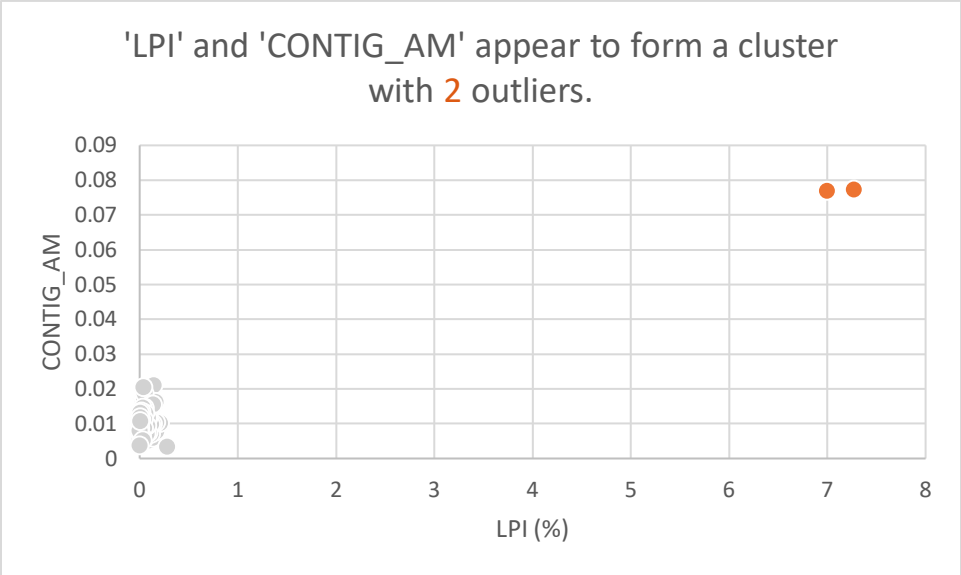

Figure B-18. Cluster between LPI and CONTIG_AM

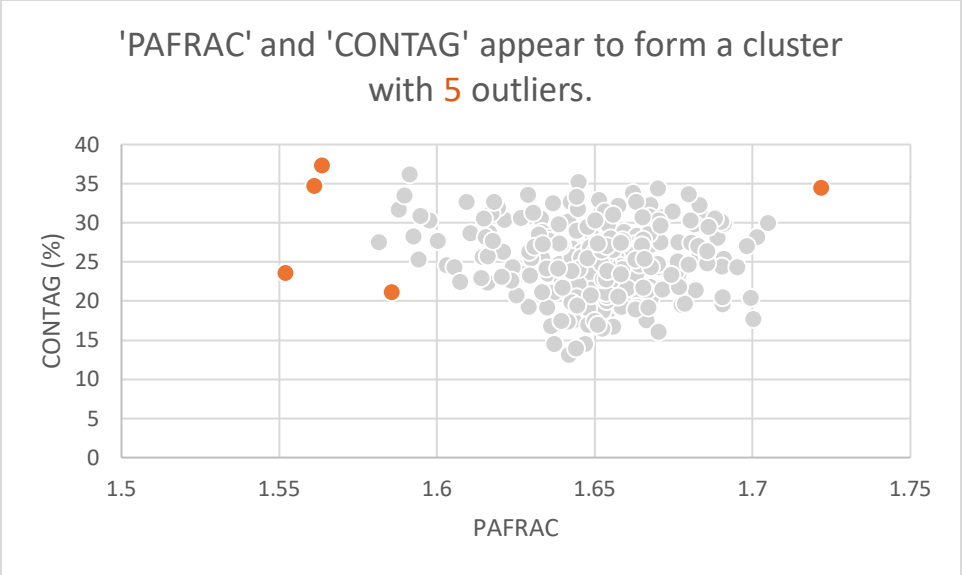

Figure B-19. Cluster between PAFRAC and CONTAG

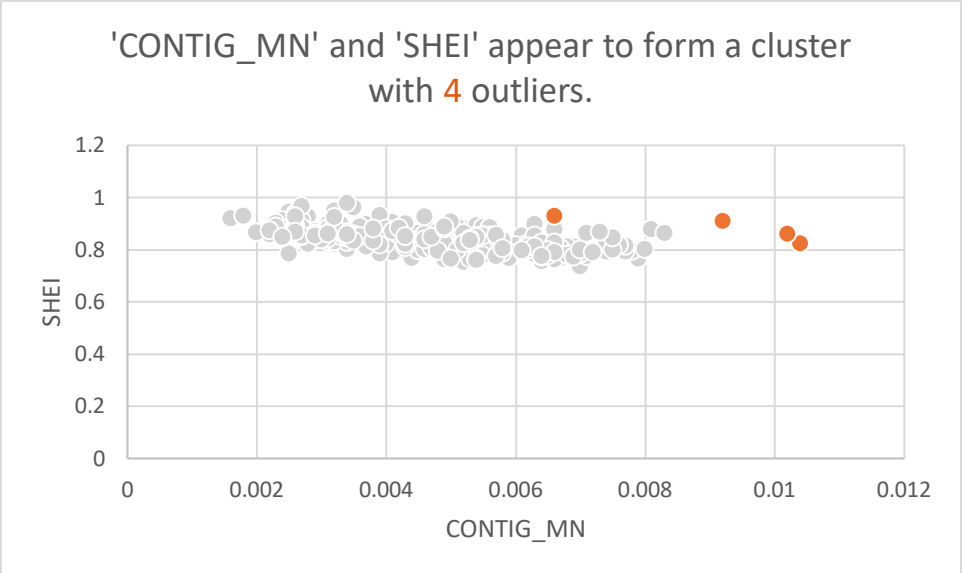

Figure B-20. Cluster between CONTIG_MN and SHEI

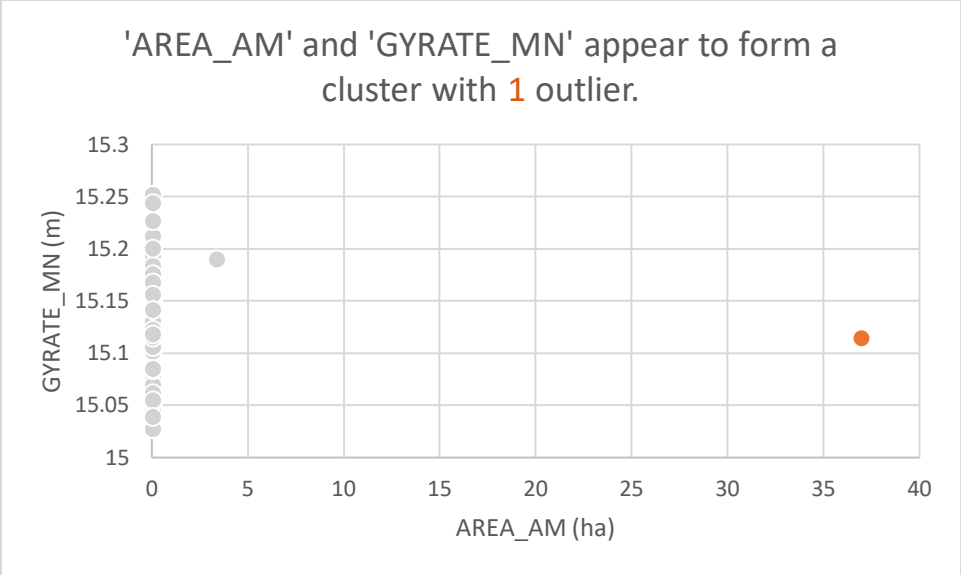

Figure B-21. Cluster between AREA_AM and GYRATE_MN

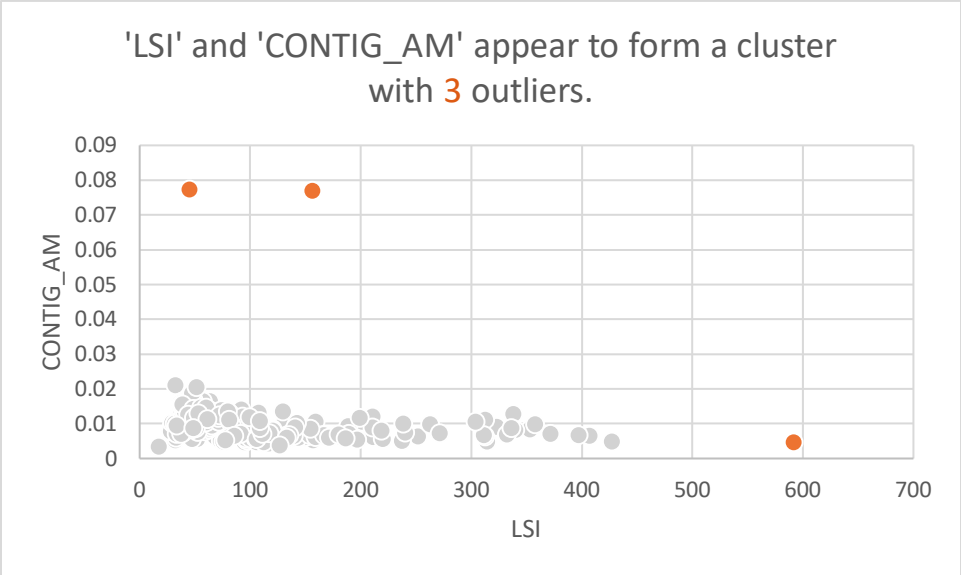

Figure B-22. Cluster between LSI and CONTIG_AM

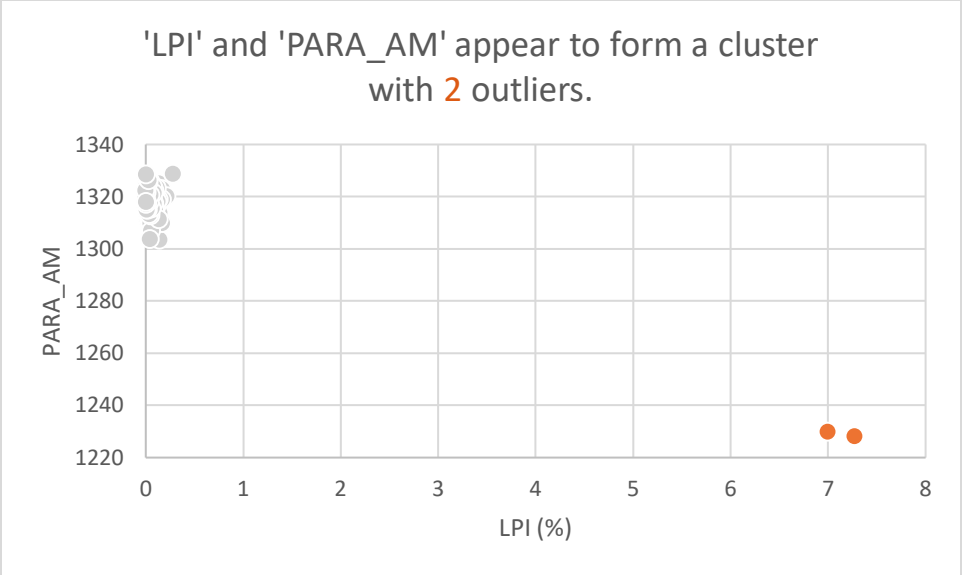

Figure B-23. Cluster between LPI and PARA_AM

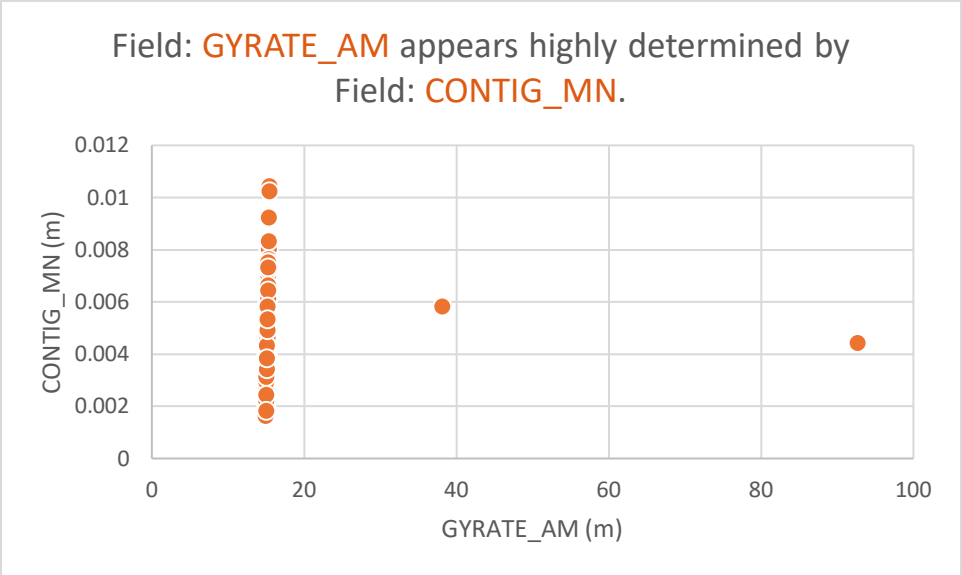

Figure B-24. Highly Determined between GYRATE_AM and CONTIG_MN

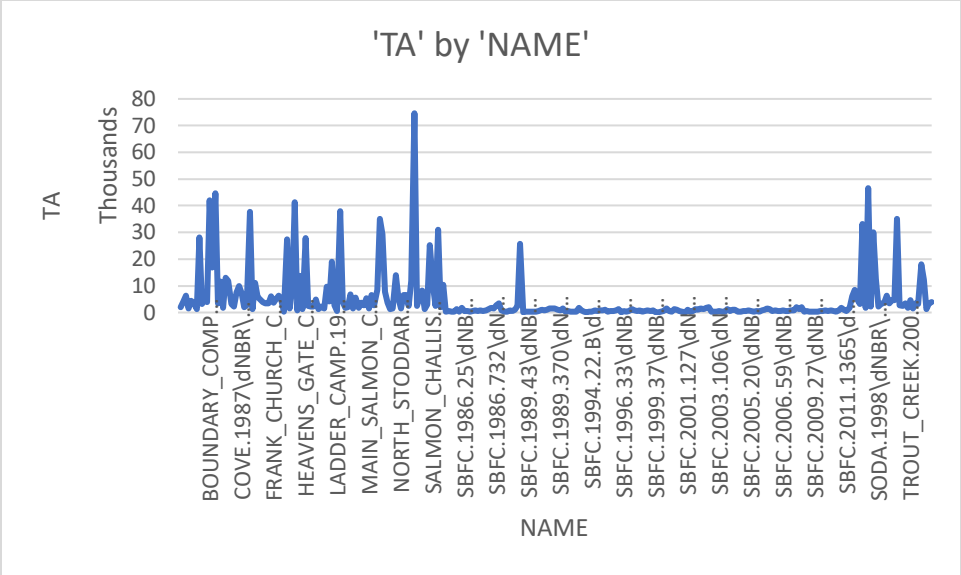

Figure B-25. Total Area (TA) of some of the largest fires by name.

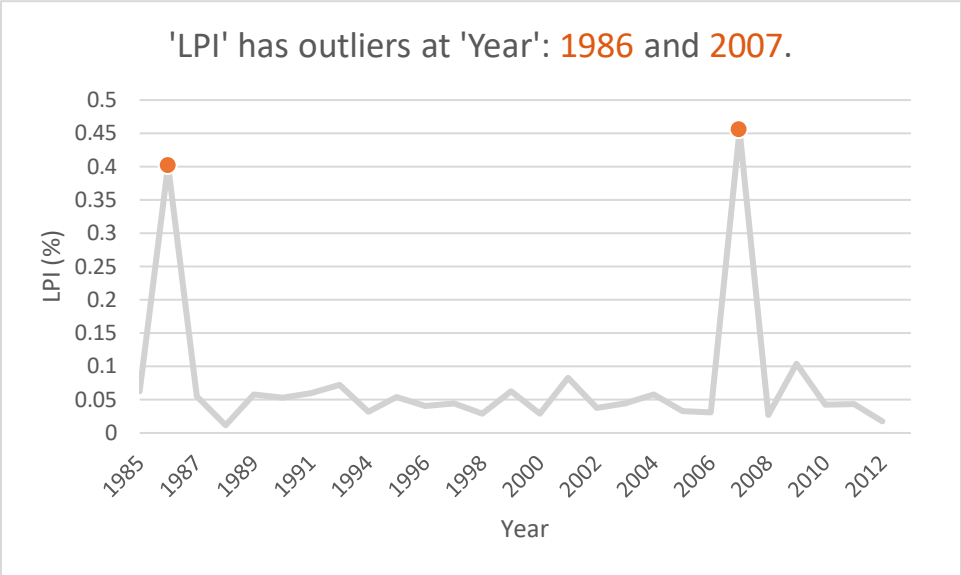

Figure B-26. Two outliers of fire peaks according to the LPI metric.

APPENDIX C

Table of average LPI by year

Table 3. Average most extensive patch index (LPI) values from 1985-2012

Row Labels	Average of LPI
1985	0.062644444
1986	0.40187
1987	0.05505
1988	0.01158
1989	0.058027778
1990	0.05318
1991	0.0595
1992	0.072425
1994	0.03155
1995	0.054016667
1996	0.040761538
1997	0.044033333
1998	0.02925
1999	0.062338462
2000	0.0285125
2001	0.08316
2002	0.037511111
2003	0.044533333
2004	0.05815
2005	0.032313636
2006	0.030995455
2007	0.45481875
2008	0.027342857
2009	0.1035
2010	0.0427
2011	0.043111111
2012	0.01765
Grand Total	0.091834507

APPENDIX D

Table of SHAPE_MN by year

Table 4. Average SHAPE_MN of the 296 fires from 1985-2012

Row Labels	Average of SHAPE_MN
1985	1.005388889
SBFC.1985.28\dNBR\dNBR.tif	1.0095
SBFC.1985.183\dNBR\dNBR.tif	1.0082
SBFC.1985.35\dNBR\dNBR.tif	1.0073
SBFC.1985.57\dNBR\dNBR.tif	1.0061
SBFC.1985.129\dNBR\dNBR.tif	1.005
GOAT.1985\dNBR\dNBR.tif	1.0036
FOUNTAIN.1985\dNBR\dNBR.tif	1.0035
BOISE_BAR.1985\dNBR\dNBR.tif	1.0031
SBFC.1985.340\dNBR\dNBR.tif	1.0022
1986	1.006845
SBFC.1986.59\dNBR\dNBR.tif	1.0093
SBFC.1986.60\dNBR\dNBR.tif	1.0087
SBFC.1986.27\dNBR\dNBR.tif	1.0087
SBFC.1986.34.B\dNBR\dNBR.tif	1.0086
SBFC.1986.78\dNBR\dNBR.tif	1.0085
SBFC.1986.251\dNBR\dNBR.tif	1.0075
SBFC.1986.345\dNBR\dNBR.tif	1.0073
SBFC.1985.550\dNBR\dNBR.tif	1.0073
SBFC.1986.34.A\dNBR\dNBR.tif	1.0073
HAND_MEADOWS.1986\dNBR\dNBR.tif	1.0071
SBFC.1986.25\dNBR\dNBR.tif	1.0071
SBFC.1986.349\dNBR\dNBR.tif	1.0069
SBFC.1986.1023\dNBR\dNBR.tif	1.0068
SBFC.1986.70\dNBR\dNBR.tif	1.0068
SBFC.1986.732\dNBR\dNBR.tif	1.0064
SBFC.1986.33\dNBR\dNBR.tif	1.0063
DEVILS_TEETH.1986\dNBR\dNBR.tif	1.0058
TENNESSEE_CREEK.1986\dNBR\dNBR.tif	1.0039

LITTLE_SQUAW.1986\dNBR\dNBR.tif	1.0036
MULE_CRK_POINT.1986\dNBR\dNBR.tif	1.003
1987	1.0050625
SBFC.1987.32\dNBR\dNBR.tif	1.0066
SBFC.1987.50\dNBR\dNBR.tif	1.0061
SBFC.1987.201\dNBR\dNBR.tif	1.0061
COVE.1987\dNBR\dNBR.tif	1.006
DEADWOOD.1987\dNBR\dNBR.tif	1.0046
SBFC.1987.250\dNBR\dNBR.tif	1.0041
TAPPAN_CREEK.1987\dNBR\dNBR.tif	1.0039
SBFC.1987.90\dNBR\dNBR.tif	1.0031
1988	1.00425
CAMP_LADDER.1988\dNBR\dNBR.tif	1.0061
SBFC.1988.14248\dNBR\dNBR.tif	1.0059
LADDER_HIDA_PT.1988\dNBR\dNBR.tif	1.0056
LADDER_CAMP.1988\dNBR\dNBR.tif	1.0041
SBFC.1988.1168\dNBR\dNBR.tif	1.0039
MCCARTE_RIDGE.1988\dNBR\dNBR.tif	1.0037
SLIVER_CREEK.1988\dNBR\dNBR.tif	1.0037
GOLDEN.1988\dNBR\dNBR.tif	1.0037
SBFC.1988.75\dNBR\dNBR.tif	1.003
CABIN.1988\dNBR\dNBR.tif	1.0028
1989	1.005338889
SBFC.1989.180\dNBR\dNBR.tif	1.0079
SBFC.1989.69\dNBR\dNBR.tif	1.0077
SBFC.1989.77\dNBR\dNBR.tif	1.0068
SBFC.1989.210\dNBR\dNBR.tif	1.0064
SBFC.1989.313\dNBR\dNBR.tif	1.0063
SBFC.1989.150\dNBR\dNBR.tif	1.0058
SBFC.1989.45\dNBR\dNBR.tif	1.0057
SBFC.1989.51\dNBR\dNBR.tif	1.0052
SBFC.1989.44\dNBR\dNBR.tif	1.0051

SBFC.1989.341\dNBR\dNBR.tif	1.0051
SBFC.1989.456\dNBR\dNBR.tif	1.0049
SBFC.1989.41\dNBR\dNBR.tif	1.0048
SBFC.1989.33\dNBR\dNBR.tif	1.0048
SBFC.1989.43\dNBR\dNBR.tif	1.0048
SBFC.1989.344\dNBR\dNBR.tif	1.0047
SBFC.1989.370\dNBR\dNBR.tif	1.0041
JOHNSON_BUTTE.1989\dNBR\dNBR.tif	1.0033
GAME_CREEK.1989\dNBR\dNBR.tif	1.0027
1990	1.00553
SBFC.1990.38\dNBR\dNBR.tif	1.0076
SBFC.1990.31\dNBR\dNBR.tif	1.0076
SBFC.1990.401\dNBR\dNBR.tif	1.0068
WILDHORSE_CREEK.1990\dNBR\dNBR.tif	1.0056
SBFC.1990.411\dNBR\dNBR.tif	1.0054
SBFC.1990.59\dNBR\dNBR.tif	1.0053
SBFC.1990.20.B\dNBR\dNBR.tif	1.0052
CHAMBERLAIN.1990\dNBR\dNBR.tif	1.0051
SBFC.1990.101\dNBR\dNBR.tif	1.0046
SABE_CREEK.1990\dNBR\dNBR.tif	1.0021
1991	1.006166667
SBFC.1991.30.B\dNBR\dNBR.tif	1.0116
RUSH_CREEK.1991\dNBR\dNBR.tif	1.004
KITCHEN.1991\dNBR\dNBR.tif	1.0029
1992	1.004625
SBFC.1992.87\dNBR\dNBR.tif	1.005
PORCUPINE.TOMATO.1992\dNBR\dNBR.tif	1.0048
SBFC.1992.31\dNBR\dNBR.tif	1.0046
LAKE.1992\dNBR\dNBR.tif	1.0041
1994	1.00383
SBFC.1994.104\dNBR\dNBR.tif	1.0053
SBFC.1994.256\dNBR\dNBR.tif	1.0048

SBFC.1994.377\dNBR\dNBR.tif	1.0044
SBFC.1994.22.B\dNBR\dNBR.tif	1.0042
SBFC.1994.170\dNBR\dNBR.tif	1.0042
SBFC.1994.303\dNBR\dNBR.tif	1.0038
PIONEER_COMPLEX_PIONEER_CREEK.1994\dNBR\dNBR.tif	1.0034
TAG.1994\dNBR\dNBR.tif	1.0029
BITTER-NEZ_COMPLEX_MAGRUDER.1994\dNBR\dNBR.tif	1.0027
PORPHYRY_SOUTH.1994\dNBR\dNBR.tif	1.0026
1995	1.00675
SBFC.1995.80\dNBR\dNBR.tif	1.0093
SBFC.1995.24\dNBR\dNBR.tif	1.0077
SBFC.1995.199\dNBR\dNBR.tif	1.0068
SBFC.1995.21\dNBR\dNBR.tif	1.0068
SBFC.1995.61\dNBR\dNBR.tif	1.0057
WATERFALL.1995\dNBR\dNBR.tif	1.0042
1996	1.004707692
SBFC.1996.182\dNBR\dNBR.tif	1.0071
SBFC.1996.29\dNBR\dNBR.tif	1.0064
SBFC.1996.125\dNBR\dNBR.tif	1.0057
SBFC.1996.97\dNBR\dNBR.tif	1.0056
SBFC.1996.207\dNBR\dNBR.tif	1.0051
STODDARD.1996\dNBR\dNBR.tif	1.005
SWET-WARRIOR_COMPLEX_SWET_CREEK.1996\dNBR\dNBR.tif	1.005
SBFC.1996.33\dNBR\dNBR.tif	1.0049
FALCONBERRY.1996\dNBR\dNBR.tif	1.004
BRIDGE.1996\dNBR\dNBR.tif	1.0037
HARRINGTON.1996\dNBR\dNBR.tif	1.0033
BIG_BRUIN.1996\dNBR\dNBR.tif	1.0028
SWET-WARRIOR_COMPLEX_WARRIORS_FACE.1996\dNBR\dNBR.tif	1.0026
1997	1.006366667
SBFC.1997.75\dNBR\dNBR.tif	1.008
SBFC.1997.27\dNBR\dNBR.tif	1.008

COLT.1997\dNBR\dNBR.tif	1.0031
1998	1.004628571
SBFC.1998.75\dNBR\dNBR.tif	1.0081
SBFC.1998.29\dNBR\dNBR.tif	1.0079
SBFC.1998.59\dNBR\dNBR.tif	1.0056
MAIN_SALMON_COMPLEX_BEND_CREEK.1998\dNBR\dNBR.tif	1.0047
SBFC.1998.92\dNBR\dNBR.tif	1.0047
ROCK_RABBIT.1998\dNBR\dNBR.tif	1.0046
SODA.1998\dNBR\dNBR.tif	1.0043
JACKASS.1998\dNBR\dNBR.tif	1.0042
MAIN_SALMON_COMPLEX_COLT.1998\dNBR\dNBR.tif	1.004
MAIN_SALMON_COMPLEX_RAINIER.1998\dNBR\dNBR.tif	1.0036
MAIN_SALMON_COMPLEX_HAMILTON.1998\dNBR\dNBR.tif	1.0036
LAID_LOW.1998\dNBR\dNBR.tif	1.0033
ARCTIC_CREEK.1998\dNBR\dNBR.tif	1.0033
MAIN_SALMON_COMPLEX_CAYUSE.1998\dNBR\dNBR.tif	1.0029
1999	1.004776923
LODGEPOLE.1999\dNBR\dNBR.tif	1.0074
SBFC.1999.34\dNBR\dNBR.tif	1.0074
SOLDIER_IRIS.1999\dNBR\dNBR.tif	1.0068
SBFC.1999.394\dNBR\dNBR.tif	1.0059
SBFC.1999.41\dNBR\dNBR.tif	1.0056
SBFC.1999.37\dNBR\dNBR.tif	1.0056
DEVIL_STORM.1999\dNBR\dNBR.tif	1.0042
FLOYDS_COMPLEX_LITTLE_RAMEY.1999\dNBR\dNBR.tif	1.004
NORTON_CREEK.1999\dNBR\dNBR.tif	1.0038
FLOYDS_COMPLEX_COPPER_CAMP.1999\dNBR\dNBR.tif	1.0038
SOLDIER_SOLDIER.1999\dNBR\dNBR.tif	1.0034
SBFC.1999.129\dNBR\dNBR.tif	1.0028
SBFC.1999.39\dNBR\dNBR.tif	1.0014
2000	1.003975
SBFC.2000.234\dNBR\dNBR.tif	1.0075

SBFC.2000.27\dNBR\dNBR.tif	1.0065
SBFC.2000.282\dNBR\dNBR.tif	1.0065
WILDERNESS_COMPLEX_HAMILTON.2000\dNBR\dNBR.tif	1.0055
WILDERNESS_COMPLEX_LONELY.2000\dNBR\dNBR.tif	1.0042
BLACK_LAKE.2000\dNBR\dNBR.tif	1.004
GRASS_MOUNTAIN.2000\dNBR\dNBR.tif	1.0037
SALMON_CHALLIS_WILDERNESS_COMPLEX_LITTLE_PISTOL.2000\dNBR\dNBR.tif	1.0035
SBFC.2000.93\dNBR\dNBR.tif	1.0034
SALMON_CHALLIS_WILDERNESS_COMPLEX_BUTTS.2000\dNBR\dNBR.tif	1.0031
SALMON_CHALLIS_WILDERNESS_COMPLEX_PACKER_MEADOW.2000\dNBR\dNBR.tif	1.0031
SALMON_CHALLIS_WILDERNESS_COMPLEX_FILLY.2000\dNBR\dNBR.tif	1.0027
KITCHEN.2000\dNBR\dNBR.tif	1.0027
WILDERNESS_COMPLEX_SHORT_CREEK.2000\dNBR\dNBR.tif	1.0026
BURGDORF_JUNCTION.2000\dNBR\dNBR.tif	1.0026
YELLOWPINE_COMPLEX_INDIAN_and_PROSPECT.2000\dNBR\dNBR.tif	1.002
2001	1.00596
SBFC.2001.30\dNBR\dNBR.tif	1.0083
SBFC.2001.33\dNBR\dNBR.tif	1.0082
SBFC.2001.127\dNBR\dNBR.tif	1.0054
SBFC.2001.38\dNBR\dNBR.tif	1.0049
SNOWSHOE.2001\dNBR\dNBR.tif	1.003
2002	1.006233333
SBFC.2002.195\dNBR\dNBR.tif	1.0096
SBFC.2002.142\dNBR\dNBR.tif	1.0079
SBFC.2002.231\dNBR\dNBR.tif	1.0074
SBFC.2002.371\dNBR\dNBR.tif	1.0069
SBFC.2002.254\dNBR\dNBR.tif	1.0063
SBFC.2002.148\dNBR\dNBR.tif	1.0063
SBFC.2002.129\dNBR\dNBR.tif	1.0061
SBFC.2002.43\dNBR\dNBR.tif	1.0028
FRANK_CHURCH_COMPLEX_LITTLE_HORSE.2002\dNBR\dNBR.tif	1.0028
2003	1.004827778

SBFC.2003.307\dNBR\dNBR.tif	1.0072
SBFC.2003.27\dNBR\dNBR.tif	1.007
SAPP_RICHARDSON.2003\dNBR\dNBR.tif	1.0064
SBFC.2003.106\dNBR\dNBR.tif	1.0057
SBFC.2003.33.B\dNBR\dNBR.tif	1.0056
SBFC.2003.378\dNBR\dNBR.tif	1.0056
SBFC.2003.354\dNBR\dNBR.tif	1.0055
SBFC.2003.151\dNBR\dNBR.tif	1.0053
NORTH_STODDARD.2003\dNBR\dNBR.tif	1.0045
SBFC.2003.314\dNBR\dNBR.tif	1.0044
MIDDLE_FORK_COMPLEX_RUSH.2003\dNBR\dNBR.tif	1.0043
SBFC.2003.38\dNBR\dNBR.tif	1.0038
MIDDLE_FORK_COMPLEX_FALCONBERRY.2003\dNBR\dNBR.tif	1.0038
MIDDLE_FORK_COMPLEX_PROSPECT.2003\dNBR\dNBR.tif	1.0038
SBFC.2003.114\dNBR\dNBR.tif	1.0038
CRYSTAL_CREEK.2003\dNBR\dNBR.tif	1.0036
SLIMS_COMPLEX_POET.2003\dNBR\dNBR.tif	1.0035
NORTH_FORK_LICK_MARBLE.2003\dNBR\dNBR.tif	1.0031
2004	1.005466667
SBFC.2004.62\dNBR\dNBR.tif	1.0068
SBFC.2004.66\dNBR\dNBR.tif	1.0066
SBFC.2004.213\dNBR\dNBR.tif	1.0061
SBFC.2004.104\dNBR\dNBR.tif	1.0051
SBFC.2004.171\dNBR\dNBR.tif	1.0048
PORTER_WFU.2004\dNBR\dNBR.tif	1.0034
2005	1.0056
SBFC.2005.149\dNBR\dNBR.tif	1.0097
SBFC.2005.34\dNBR\dNBR.tif	1.0088
SBFC.2005.35\dNBR\dNBR.tif	1.0084
SBFC.2005.280\dNBR\dNBR.tif	1.0082
SBFC.2005.49\dNBR\dNBR.tif	1.0077
SBFC.2005.20\dNBR\dNBR.tif	1.0068

FRANK_CHURCH_WFU_WEST_FORK_AND_JOE.2005\dNBR\dNBR.tif	1.0066
SBFC.2005.55\dNBR\dNBR.tif	1.0065
FRANK_CHURCH_WFU_WEST_FORK_AND_JOE.WOLFFANG.2005\dNBR\dNBR.tif	1.0062
SBFC.2005.371\dNBR\dNBR.tif	1.0059
LOWER_BURN_CREEK.2005\dNBR\dNBR.tif	1.005
STODDARD_CREEK_POINT.2005\dNBR\dNBR.tif	1.005
SELWAY-SALMON_COMPLEX_REYNOLDS_LAKE.2005\dNBR\dNBR.tif	1.0047
MARBLE.2005\dNBR\dNBR.tif	1.0042
NINE_SHOT_WFU.2005\dNBR\dNBR.tif	1.0042
STRIPE_CREEK.2005\dNBR\dNBR.tif	1.0038
FRANK_CHURCH_WFU_ROOT_CREEK.2005\dNBR\dNBR.tif	1.0038
FRANK_CHURCH_WFU_BEAR_CREEK.2005\dNBR\dNBR.tif	1.0037
FRANK_CHURCH_WFU_MISSOURI_RIDGE.2005\dNBR\dNBR.tif	1.0036
BURNT_STRIP_MOUNTAIN.2005\dNBR\dNBR.tif	1.0036
MUSTANG_WFU.2005\dNBR\dNBR.tif	1.0034
SELWAY-SALMON_COMPLEX_BEAVERJACK.2005\dNBR\dNBR.tif	1.0034
2006	1.0067
SBFC.2006.111\dNBR\dNBR.tif	1.0109
SBFC.2006.73\dNBR\dNBR.tif	1.0103
SBFC.2006.59\dNBR\dNBR.tif	1.0099
SBFC.2006.28.B\dNBR\dNBR.tif	1.0088
SBFC.2006.44\dNBR\dNBR.tif	1.0086
SBFC.2006.115\dNBR\dNBR.tif	1.0086
SBFC.2006.21.A\dNBR\dNBR.tif	1.0081
SBFC.2006.46\dNBR\dNBR.tif	1.0077
SHELDON_PEAK.2006\dNBR\dNBR.tif	1.0074
MIDDLE_FORK_COMPLEX.2006\dNBR\dNBR.tif	1.0072
SBFC.2006.221\dNBR\dNBR.tif	1.007
SBFC.2006.355\dNBR\dNBR.tif	1.0064
LEWIS_WFU.2006\dNBR\dNBR.tif	1.0064
SBFC.2006.64\dNBR\dNBR.tif	1.0063
CUB.2006\dNBR\dNBR.tif	1.0062

SBFC.2006.822\dNBR\dNBR.tif	1.0054
DUNCE_WFU.2006\dNBR\dNBR.tif	1.0045
BOUNDARY_COMPLEX.2006\dNBR\dNBR.tif	1.0041
SOUTHFORK_COMPLEX_BISHOP_CREEK.2006\dNBR\dNBR.tif	1.0037
BURNT.2006\dNBR\dNBR.tif	1.0037
TROUT_CREEK.2006\dNBR\dNBR.tif	1.0035
HEAVENS_GATE_COMPLEX_BLACK_BUTTE.2006\dNBR\dNBR.tif	1.0027
2007	1.0050375
BITTERROOT_FIRE_USE_COMPLEX_MAGRUDER_MTN1_3.2007\dNBR\dNBR.tif	1.0075
SBFC.2007.52\dNBR\dNBR.tif	1.0067
SHOWER_BATH_COMPLEX_RED_BLUFF_2.2007\dNBR\dNBR.tif	1.0057
KRASSEL_COMPLEX_GOAT_WFU_2.2007\dNBR\dNBR.tif	1.0055
EAST_ZONE_COMPLEX_RAINES_2.2007\dNBR\dNBR.tif	1.0054
BITTERROOT_FIRE_USE_CX_MAGRUDER_MTN1_6.7.KRASSEL.TAG.2007\dNBR\dNBR.tif	1.005
BITTERROOT_FIRE_USE_COMPLEX_MAGRUDER_MTN1_2.2007\dNBR\dNBR.tif	1.005
CONFLUENCE_COMPLEX_CLEAR_SAGE.2007\dNBR\dNBR.tif	1.0048
KRASSEL_COMPLEX_COTTONWOOD_WFU_2.2007\dNBR\dNBR.tif	1.0048
KRASSEL_COMPLEX_TAG_WFU_1.2007\dNBR\dNBR.tif	1.0047
KRASSEL_COMPLEX_GOAT_WFU_1.2007\dNBR\dNBR.tif	1.0046
SHOWER_BATH_COMPLEX_RED_BLUFF_1.2007\dNBR\dNBR.tif	1.0044
SBFC.2007.186\dNBR\dNBR.tif	1.0044
KRASSEL_COMPLEX_COTTONWOOD_WFU_1.2007\dNBR\dNBR.tif	1.0042
CONFLUENCE_COMPLEX_PAPOOSE_WFU.2007\dNBR\dNBR.tif	1.0042
SHOWER_BATH_COMPLEX_SHOWER_BATH.2007\dNBR\dNBR.tif	1.0037
2008	1.005385714
CABIN CREEK.2008\dNBR\dNBR.tif	1.008
SBFC.2008.81\dNBR\dNBR.tif	1.0062
PORCUPINE.2008\dNBR\dNBR.tif	1.0061
RUSH_CREEK_1.2008\dNBR\dNBR.tif	1.0059
WESTY_1.2008\dNBR\dNBR.tif	1.0052
HELLS_HALF_SADDLE.2008\dNBR\dNBR.tif	1.0036
BORDER_COMPLEX_CAYUSE.2008\dNBR\dNBR.tif	1.0027

2009	1.0081
SBFC.2009.20.B\dNBR\dNBR.tif	1.0091
SBFC.2009.51\dNBR\dNBR.tif	1.0082
SBFC.2009.28\dNBR\dNBR.tif	1.0078
SBFC.2009.27\dNBR\dNBR.tif	1.0073
2010	1.006085714
SBFC.2010.230\dNBR\dNBR.tif	1.0085
SBFC.2010.23\dNBR\dNBR.tif	1.0082
SBFC.2010.94\dNBR\dNBR.tif	1.0077
SBFC.2010.175\dNBR\dNBR.tif	1.0066
BIGHORN.2010\dNBR\dNBR.tif	1.0045
BANNER.2010\dNBR\dNBR.tif	1.0037
LITTLE_BEAVER_COMPLEX.2010\dNBR\dNBR.tif	1.0034
2011	1.0054
SBFC.2011.177\dNBR\dNBR.tif	1.0078
SBFC.2011.138\dNBR\dNBR.tif	1.0074
SBFC.2011.251\dNBR\dNBR.tif	1.0062
SBFC.2011.31\dNBR\dNBR.tif	1.0061
HELLS_HALF_COMPLEX.2011\dNBR\dNBR.tif	1.0061
SBFC.2011.1365\dNBR\dNBR.tif	1.004
SADDLE_COMPLEX.2011\dNBR\dNBR.tif	1.004
SBFC.2011.29\dNBR\dNBR.tif	1.004
VELVET.2011\dNBR\dNBR.tif	1.003
2012	1.00645
SBFC.2012.451\dNBR\dNBR.tif	1.0079
SBFC.2012.3886\dNBR\dNBR.tif	1.005
Grand Total	1.00541338

APPENDIX E

Pearson Correlation Matrix (PCM)

The matrix is also available in the supplemental excel file. Figures were not evaluated.

	TA	NP	PD	LPI	ED	LSI	AREA_MN	AREA_AM	AREA_CV	GYRATE_MN	GYRATE_AM	GYRATE_CV	SHAPE_MN	SHAPE_AM	SHAPE_CV
TA	1.0***	1.0***	0.36*	0.32	-0.22	0.86***	-0.36*	0.47**	0.43**	-0.43**	0.44**	-0.21	-0.45**	-0.34*	-0.45**
NP	1.0***	1.0***	0.37*	0.32	-0.22	0.86***	-0.37*	0.47**	0.42**	-0.44**	0.43**	-0.22	-0.45**	-0.34*	-0.45**
PD	0.36*	0.37*	1.0***	-0.28	0.41**	0.51***	-1.0***	-0.07	-0.19	-0.98***	-0.17	-0.94***	-0.97***	-0.99***	-0.98***
LPI	0.32	0.32	-0.28	1.0***	-0.31	0.18	0.28	0.73***	0.84***	0.13	0.84***	0.55***	0.12	0.35*	0.14
ED	-0.22	-0.22	0.41**	-0.31	1.0***	-0.18	-0.4**	-0.29	-0.34*	-0.37*	-0.33*	-0.46**	-0.38*	-0.43**	-0.38**
LSI	0.86***	0.86***	0.51***	0.18	-0.18	1.0***	-0.51***	0.35*	0.29	-0.57***	0.3	-0.38**	-0.59***	-0.5***	-0.59***
AREA_MN	-0.36*	-0.37*	-1.0***	0.28	-0.4**	-0.51***	1.0***	0.07	0.19	0.98***	0.17	0.94***	0.97***	0.99***	0.97***
AREA_AM	0.47**	0.47**	-0.07	0.73***	-0.29	0.35*	0.07	1.0***	0.98***	-0.07	0.98***	0.32	-0.08	0.13	-0.06
AREA_CV	0.43**	0.42**	-0.19	0.84***	-0.34*	0.29	0.19	0.98***	1.0***	0.05	1.0***	0.45**	0.03	0.25	0.05
GYRATE_MN	-0.43**	-0.44**	-0.98***	0.13	-0.37*	-0.57***	0.98***	-0.07	0.05	1.0***	0.03	0.89***	1.0***	0.97***	0.99***
GYRATE_AM	0.44**	0.43**	-0.17	0.84***	-0.33*	0.3	0.17	0.98***	1.0***	0.03	1.0***	0.43**	0.01	0.24	0.03
GYRATE_CV	-0.21	-0.22	-0.94***	0.55***	-0.46**	-0.38**	0.94***	0.32	0.45**	0.89***	0.43**	1.0***	0.88***	0.97***	0.9***
SHAPE_MN	-0.45**	-0.45**	-0.97***	0.12	-0.38*	-0.59***	0.97***	-0.08	0.03	1.0***	0.01	0.88***	1.0***	0.97***	0.99***
SHAPE_AM	-0.34*	-0.34*	-0.99***	0.35*	-0.43**	-0.5***	0.99***	0.13	0.25	0.97***	0.24	0.97***	0.97***	1.0***	0.97***
SHAPE_CV	-0.45**	-0.45**	-0.98***	0.14	-0.38**	-0.59***	0.97***	-0.06	0.05	0.99***	0.03	0.9***	0.99***	0.97***	1.0***
FRAC_MN	-0.45**	-0.45**	-0.98***	0.12	-0.38*	-0.58***	0.98***	-0.08	0.03	1.0***	0.01	0.88***	1.0***	0.97***	0.99***
FRAC_AM	-0.41**	-0.42**	-0.99***	0.2	-0.39**	-0.55***	0.99***	-0.01	0.11	1.0***	0.09	0.92***	0.99***	0.98***	0.99***
FRAC_CV	-0.45**	-0.45**	-0.98***	0.14	-0.39**	-0.59***	0.97***	-0.05	0.06	0.99***	0.04	0.9***	0.99***	0.97***	1.0***
PARA_MN	0.42**	0.43**	0.98***	-0.12	0.36*	0.54***	-0.98***	0.06	-0.05	-0.96***	-0.03	-0.86***	-0.96***	-0.93***	-0.96***
PARA_AM	0.17	0.17	0.93***	-0.58***	0.45**	0.33*	-0.93***	-0.36*	-0.49**	-0.85***	-0.47**	-0.97***	-0.84***	-0.93***	-0.85***
PARA_CV	-0.42**	-0.42**	-0.97***	0.15	-0.38*	-0.54***	0.97***	-0.02	0.09	0.95***	0.06	0.87***	0.94***	0.92***	0.96***
CONTIG_MN	-0.43**	-0.44**	-0.99***	0.12	-0.37*	-0.56***	0.98***	-0.07	0.04	0.98***	0.02	0.87***	0.98***	0.95***	0.98***
CONTIG_AM	-0.16	-0.17	-0.93***	0.59***	-0.46**	-0.34*	0.94***	0.36*	0.5***	0.86***	0.48**	0.98***	0.85***	0.94***	0.86***
CONTIG_CV	0.43**	0.43**	0.94***	-0.18	0.4**	0.56***	-0.93***	-0.02	-0.13	-0.91***	-0.11	-0.87***	-0.91***	-0.9***	-0.95***
PAFRAC	-0.2	-0.2	-0.17	-0.1	-0.08	-0.28	0.18	-0.16	-0.14	0.32	-0.14	0.2	0.34*	0.29	0.3
CONTAG	-0.3	-0.3	-0.04	0.08	0.43**	-0.34*	0.04	-0.08	-0.04	0.03	-0.04	0.07	0.02	0.03	0.06
PLADJ	-0.32	-0.32	-0.86***	0.41**	-0.04	-0.48**	0.87***	0.21	0.33*	0.8***	0.31	0.87***	0.79***	0.84***	0.81***
IJI	0.24	0.24	0.03	-0.08	-0.41**	0.27	-0.02	0.05	0.02	-0.01	0.02	-0.07	-0.01	-0.03	-0.05
COHESION	-0.3	-0.31	-0.99***	0.4**	-0.43**	-0.47**	0.99***	0.17	0.3	0.95***	0.28	0.98***	0.95***	0.99***	0.95***
SHEI	0.32	0.32	0.36*	-0.12	-0.3	0.46**	-0.35*	0.13	0.06	-0.38**	0.06	-0.37*	-0.38*	-0.37*	-0.4**
AI	-0.28	-0.29	-0.94***	0.51***	-0.36*	-0.45**	0.94***	0.28	0.41**	0.87***	0.39**	0.95***	0.86***	0.93***	0.87***
VPD	0.57***	0.57***	0.16	0.14	0.02	0.48**	-0.16	0.22	0.2	-0.23	0.2	-0.12	-0.25	-0.19	-0.24

	SHAPE_CV	FRAC_MN	FRAC_AM	FRAC_CV	PARA_MN	PARA_AM	PARA_CV	CONTIG_MN	CONTIG_AM	CONTIG_CV	PAFRAC	CONTAG	PLADJ	IJI	COHESION	SHEI	AI	VPD
TA	-0.45**	-0.45**	-0.41**	-0.45**	0.42**	0.17	-0.42**	-0.43**	-0.16	0.43**	-0.2	-0.3	-0.32	0.24	-0.3	0.32	-0.28	0.57***
NP	-0.45**	-0.45**	-0.42**	-0.45**	0.43**	0.17	-0.42**	-0.44**	-0.17	0.43**	-0.2	-0.3	-0.32	0.24	-0.31	0.32	-0.29	0.57***
PD	-0.98***	-0.98***	-0.99***	-0.98***	0.98***	0.93***	-0.97***	-0.99***	-0.93***	0.94***	-0.17	-0.04	-0.86***	0.03	-0.99***	0.36*	-0.94***	0.16
LPI	0.14	0.12	0.2	0.14	-0.12	-0.58***	0.15	0.12	0.59***	-0.18	-0.1	0.08	0.41**	-0.08	0.4**	-0.12	0.51***	0.14
ED	-0.38**	-0.38*	-0.39**	-0.39**	0.36*	0.45**	-0.38*	-0.37*	-0.46**	0.4**	-0.08	0.43**	-0.04	-0.41**	-0.43**	-0.3	-0.36*	0.02
LSI	-0.59***	-0.58***	-0.55***	-0.59***	0.54***	0.33*	-0.54***	-0.56***	-0.34*	0.56***	-0.28	-0.34*	-0.48**	0.27	-0.47**	0.46**	-0.45**	0.48**
AREA_MN	0.97***	0.98***	0.99***	0.97***	-0.98***	-0.93***	0.97***	0.98***	0.94***	-0.93***	0.18	0.04	0.87***	-0.02	0.99***	-0.35*	0.94***	-0.16
AREA_AM	-0.06	-0.08	-0.01	-0.05	0.06	-0.36*	-0.02	-0.07	0.36*	-0.02	-0.16	-0.08	0.21	0.05	0.17	0.13	0.28	0.22
AREA_CV	0.05	0.03	0.11	0.06	-0.05	-0.49**	0.09	0.04	0.5***	-0.13	-0.14	-0.04	0.33*	0.02	0.3	0.06	0.41**	0.2
GYRATE_MN	0.99***	1.0***	1.0***	0.99***	-0.96***	-0.85***	0.95***	0.98***	0.86***	-0.91***	0.32	0.03	0.8***	-0.01	0.95***	-0.38**	0.87***	-0.23
GYRATE_AM	0.03	0.01	0.09	0.04	-0.03	-0.47**	0.06	0.02	0.48**	-0.11	-0.14	-0.04	0.31	0.02	0.28	0.06	0.39**	0.2
GYRATE_CV	0.9***	0.88***	0.92***	0.9***	-0.86***	-0.97***	0.87***	0.87***	0.98***	-0.87***	0.2	0.07	0.87***	-0.07	0.98***	-0.37*	0.95***	-0.12
SHAPE_MN	0.99***	1.0***	0.99***	0.99***	-0.96***	-0.84***	0.94***	0.98***	0.85***	-0.91***	0.34*	0.02	0.79***	-0.01	0.95***	-0.38*	0.86***	-0.25
SHAPE_AM	0.97***	0.97***	0.98***	0.97***	-0.93***	-0.93***	0.92***	0.95***	0.94***	-0.9***	0.29	0.03	0.84***	-0.03	0.99***	-0.37*	0.93***	-0.19
SHAPE_CV	1.0***	0.99***	0.99***	1.0***	-0.96***	-0.85***	0.96***	0.98***	0.86***	-0.95***	0.3	0.06	0.81***	-0.05	0.95***	-0.4**	0.87***	-0.24
FRAC_MN	0.99***	1.0***	1.0***	0.99***	-0.97***	-0.85***	0.96***	0.99***	0.85***	-0.92***	0.29	0.03	0.8***	-0.01	0.95***	-0.37*	0.87***	-0.23
FRAC_AM	0.99***	1.0***	1.0***	0.99***	-0.97***	-0.89***	0.96***	0.98***	0.89***	-0.93***	0.28	0.04	0.83***	-0.03	0.97***	-0.39**	0.9***	-0.21
FRAC_CV	1.0***	0.99***	0.99***	1.0***	-0.96***	-0.85***	0.96***	0.98***	0.86***	-0.95***	0.3	0.07	0.81***	-0.06	0.95***	-0.41**	0.87***	-0.25
PARA_MN	-0.96***	-0.97***	-0.97***	-0.96***	1.0***	0.87***	-0.99***	-1.0***	-0.86***	0.94***	-0.07	-0.03	-0.83***	0.02	-0.95***	0.32	-0.9***	0.15
PARA_AM	-0.85***	-0.85***	-0.89***	-0.85***	0.87***	1.0***	-0.88***	-0.87***	-1.0***	0.85***	0	-0.05	-0.89***	0.05	-0.97***	0.3	-0.98***	0.04
PARA_CV	0.96***	0.96***	0.96***	0.96***	-0.99***	-0.88***	1.0***	0.98***	0.87***	-0.97***	0.02	0.08	0.85***	-0.07	0.94***	-0.34*	0.91***	-0.15
CONTIG_MN	0.98***	0.99***	0.98***	0.98***	-1.0***	-0.87***	0.98***	1.0***	0.86***	-0.94***	0.15	0.03	0.83***	-0.02	0.95***	-0.34*	0.89***	-0.18
CONTIG_AM	0.86***	0.85***	0.89***	0.86***	-0.86***	-1.0***	0.87***	0.86***	1.0***	-0.85***	0.06	0.05	0.88***	-0.05	0.97***	-0.32	0.98***	-0.06
CONTIG_CV	-0.95***	-0.92***	-0.93***	-0.95***	0.94***	0.85***	-0.97***	-0.94***	-0.85***	1.0***	-0.07	-0.15	-0.83***	0.14	-0.92***	0.39**	-0.88***	0.2
PAFRAC	0.3	0.29	0.28	0.3	-0.07	0	0.02	0.15	0.06	-0.07	1.0***	-0.04	-0.02	0.05	0.17	-0.28	-0.01	-0.37*
CONTAG	0.06	0.03	0.04	0.07	-0.03	-0.05	0.08	0.03	0.05	-0.15	-0.04	1.0***	0.35*	-0.99***	0.05	-0.73***	0.09	0.1
PLADJ	0.81***	0.8***	0.83***	0.81***	-0.83***	-0.89***	0.85***	0.83***	0.88***	-0.83***	-0.02	0.35*	1.0***	-0.34*	0.88***	-0.53***	0.92***	0
IJI	-0.05	-0.01	-0.03	-0.06	0.02	0.05	-0.07	-0.02	-0.05	0.14	0.05	-0.99***	-0.34*	1.0***	-0.04	0.73***	-0.07	-0.14
COHESION	0.95***	0.95***	0.97***	0.95***	-0.95***	-0.97***	0.94***	0.95***	0.97***	-0.92***	0.17	0.05	0.88***	-0.04	1.0***	-0.36*	0.97***	-0.14
SHEI	-0.4**	-0.37*	-0.39**	-0.41**	0.32	0.3	-0.34*	-0.34*	-0.32	0.39**	-0.28	-0.73***	-0.53***	0.73***	-0.36*	1.0***	-0.31	0.06
AI	0.87***	0.87***	0.9***	0.87***	-0.9***	-0.98***	0.91***	0.89***	0.98***	-0.88***	-0.01	0.09	0.92***	-0.07	0.97***	-0.31	1.0***	-0.07

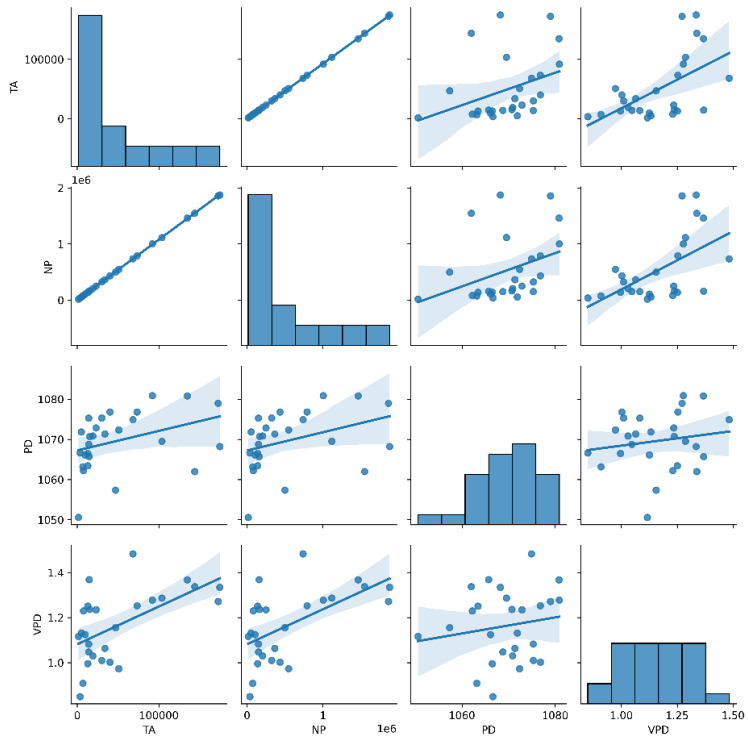

Figure E-1. VPD's linear relationship to PD, NP, and TA.

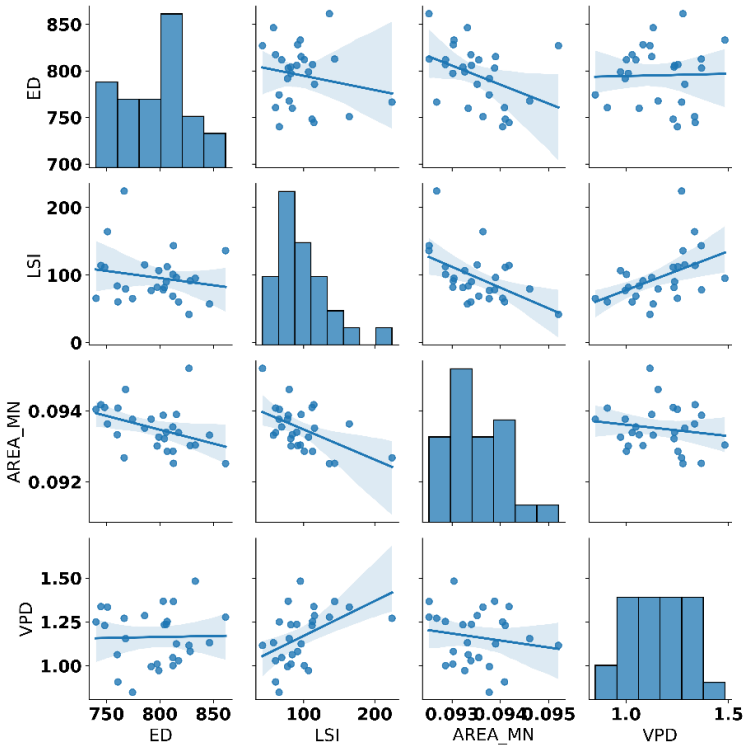

Figure E-2. VPD's linear relationship to ED, LSI, and AREA_MN.

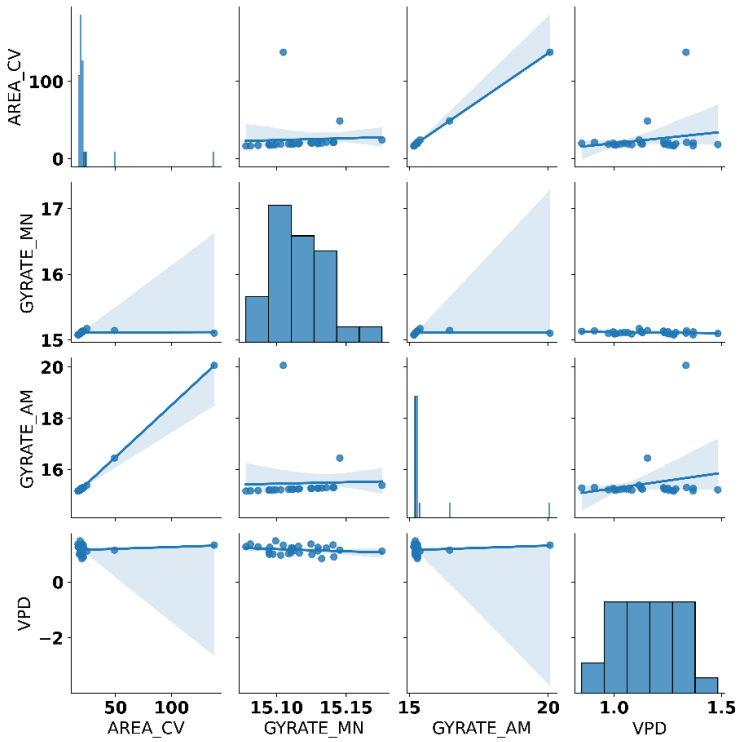

Figure E-3. VPD's linear relationship to AREA_CV, GYRATE_MN, and GYRATE_AM.

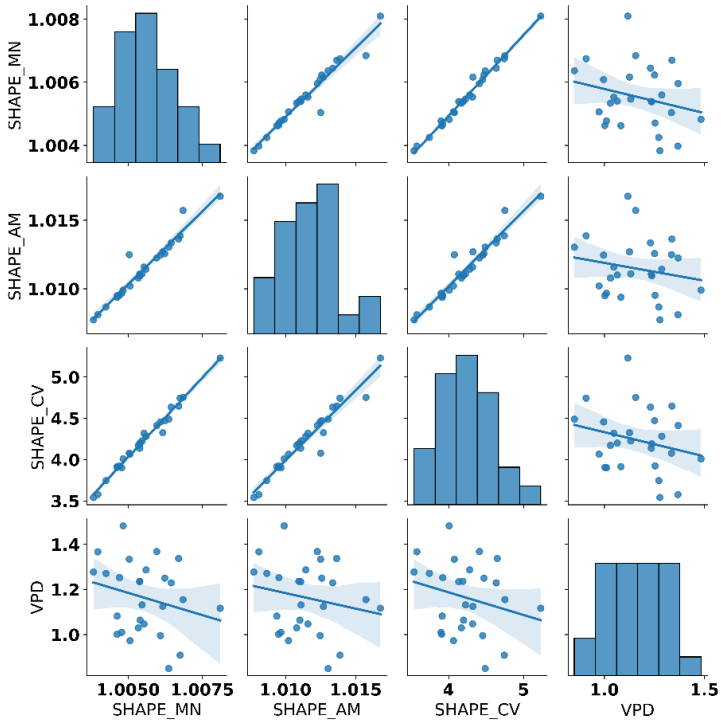

Figure E-4. VPD's linear relationship to SHAPE_MN, SHAPE_AM, and SHAPE_CV.

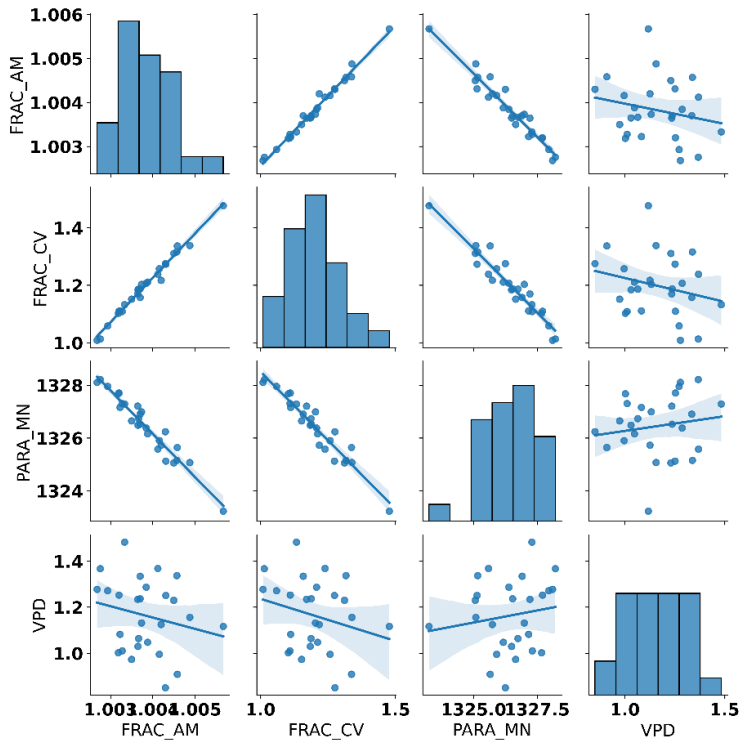

Figure E-5. VPD's linear relationship to FRAC_AM, FRAC_CV, and PARA_MN.

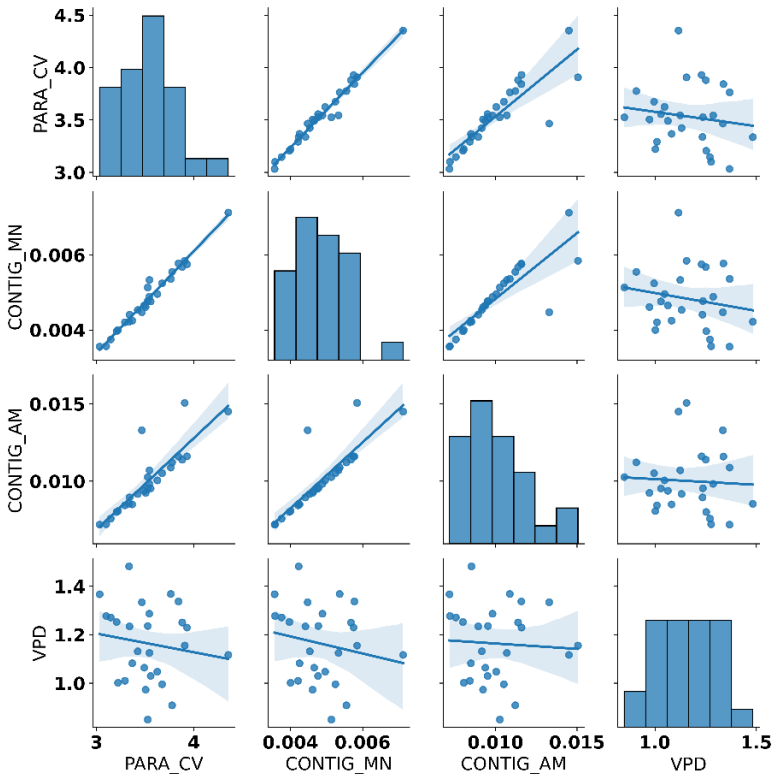

Figure E-6. VPD's linear relationship to PARA_CV, CONTIG_MN, and CONTIG_AM.

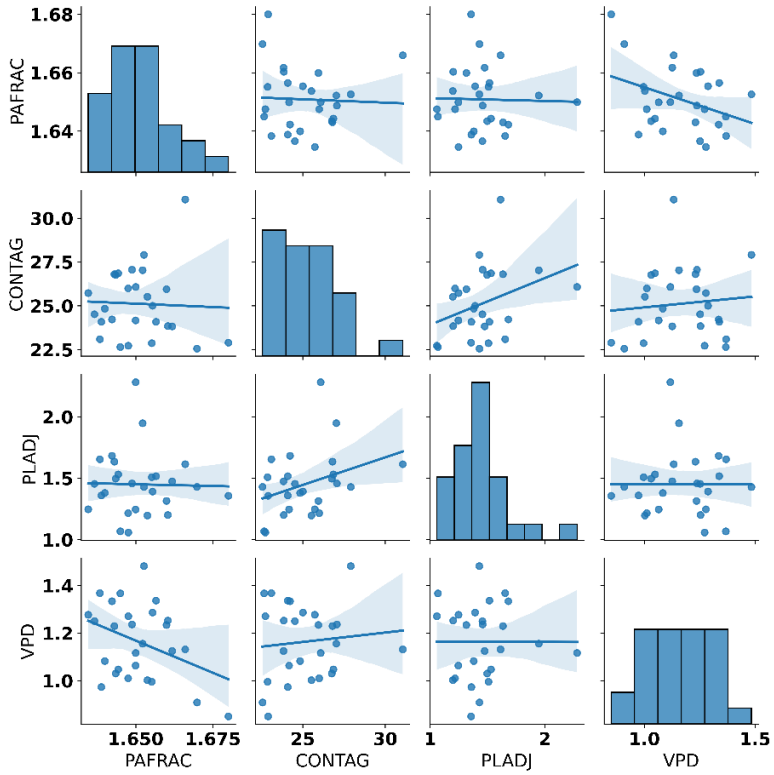

Figure E-7. VPD's linear relationship to PAFRAC, CONTAG, and PLADJ.

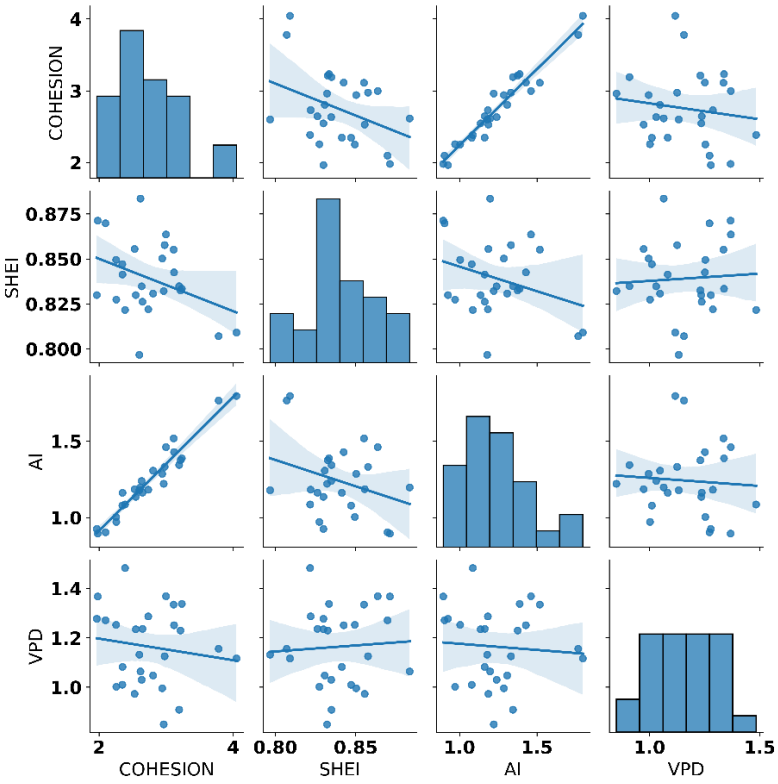

Figure E-8. VPD's linear relationship to SHEI, AI, and COHESION.

APPENDIX F

Pilot Study

The pilot study included Contagion, Patch Density, Shannon's Evenness, Mean Patch Size, and Number of Patches. I used the 8-neighbor rule, where two grid cells are part of the same patch (Gergel & Turner, 2017).

Figure 9 includes the study area and the fires I compared in the pilot study. Mustang fire burned 7/26/2005, and the post imagery was taken 7/13/2006. Arctic Creek fire burned on 7/4/1997, and the post imagery was taken on 7/26/1999. Table 5 includes the results from FRAGSTATS. The contagion values indicating the overall degree of clumping in the landscape and the differences between Arctic Creek and Mustang were 4.972, where Mustang was more significant (more clumped).

Table 5. FRAGSTATS results from a pilot study

Metric Variables	Arctic Creek (1998)	Mustang (2005)
1. Contagion	20.324	25.296
2. Patch Density	1087.256	1083.978
3. Shannon's Evenness	0.863	0.829
4. Mean Patch Size	0.014	0.016
5. Number of Patches	49907.000	13743.000

The patch density measured the size of the patches and was more significant for Arctic Creek by 3.278 per 100 ha compared to Mustang. The patch size difference indicates that the patches were more densely populated for Arctic Creek and the fire was close together and less spread out than the Mustang fire.

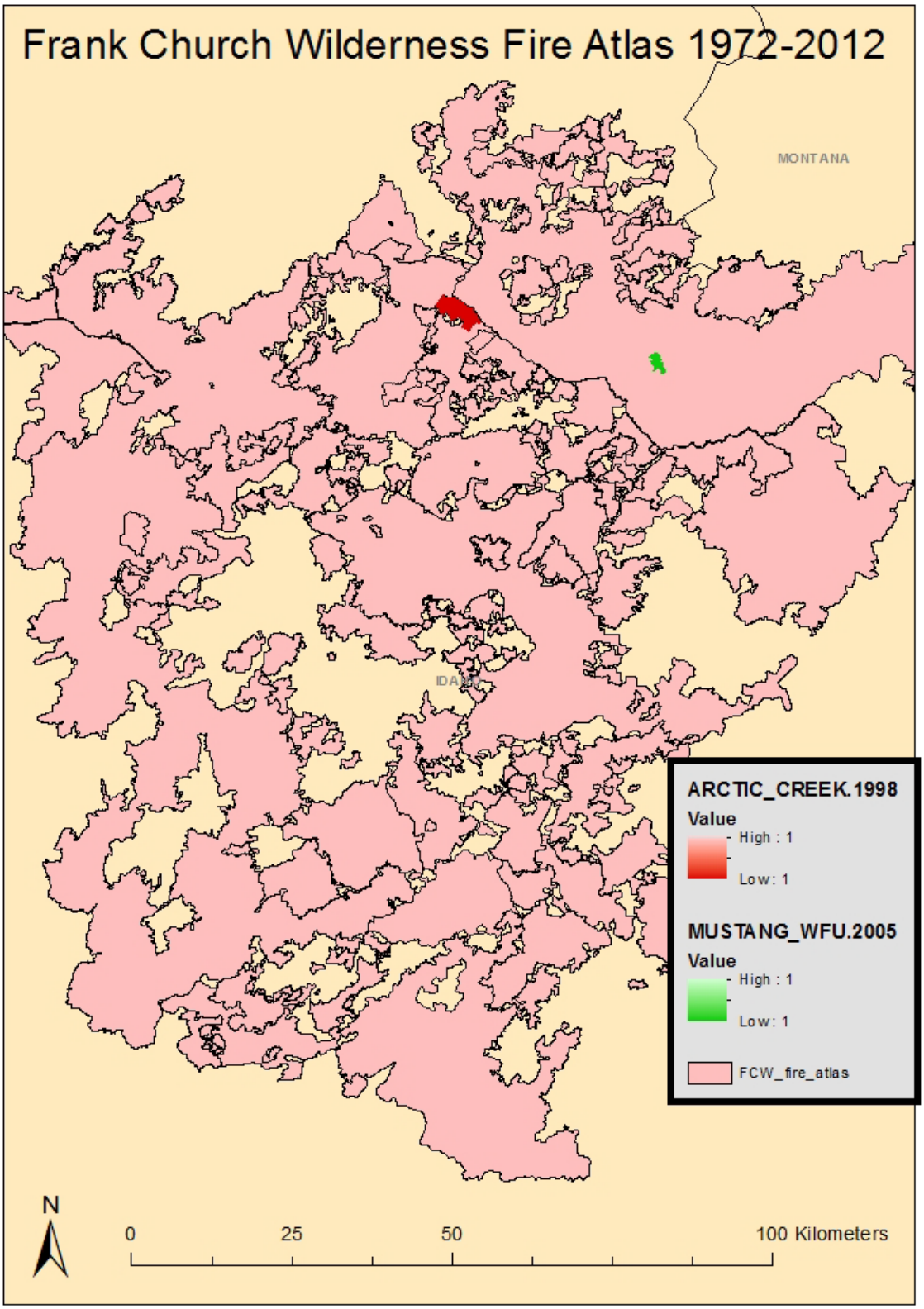

Figure F-1. The two randomly selected fire locations within the fire atlas (pilot study)

The mean patch size for the Mustang fire was higher by 0.002 compared to the Arctic Creek fire. This means the patches were more significant for the Mustang fire and that this was a larger fire as the patches that matched were larger.

The number of patches was higher for Arctic Creek by 36,164 patches compared to the Mustang fire. It has more connectedness to the patches as calculated with the 8-neighbor rule, where the patches at negligible levels are picked out.

Shannon's Evenness (SHEI) measures values of the cover type where a value near 1 indicates that the proportions of each kind are almost equal, which was the case for both fires. The SHEI was higher for Arctic Creek by 0.034 than for the Mustang fire. The difference between the fires using SHEI means the Arctic Creek fire was more even in layout than the Mustang fire; this makes sense as the time elapsed between the imagery could also indicate this (see Figure 10).

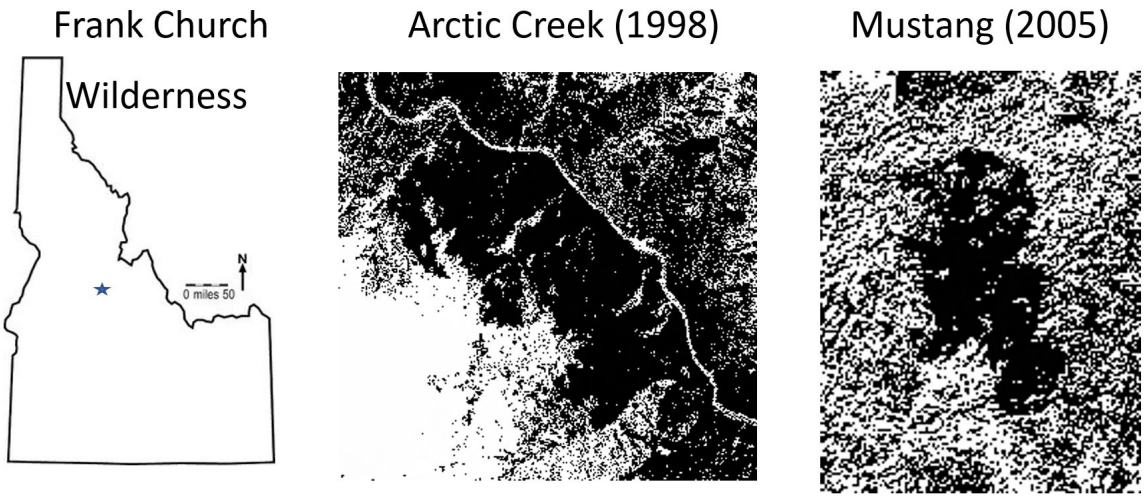

Figure F-2. Frank Church Wilderness, Idaho. The Raster (TIF) images the delta normalized difference vegetation index (dNDVI, a measure of burn severity).